Faculdade de Ciências| Faculdade de Letras| Faculdade de Medicina|
Faculdade de Psicologia

Influence of the Electrotonic Architecture on Single Neurons Dynamics: a Computational Approach

André Castro

DISSERTAÇÃO DE MESTRADO

universidade de lisboa

mestrado em ciência cognitiva

2014

Faculdade de Ciências| Faculdade de Letras| Faculdade de Medicina|
Faculdade de Psicologia

Influence of the Electrotonic Architecture on Single Neurons Dynamics: a Computational Approach

Autor:
André Castro

Projeto orientado por:
Prof. Luís Correia

DISSERTAÇÃO DE MESTRADO

UNIVERSIDADE DE LISBOA

MESTRADO EM CIÊNCIA COGNITIVA

2014

To my Mother:

She is a kind hearted woman in a hateful world who caught every thing that life ever hurled, but like the oldest mountain she always stood so tall, forever showing what it means to be unbreakable. She was the one who taught the sun to shine... She is the person I aspire to be.

Acknowledgements

First and foremost, I would like to thank my supervisor Professor Luís Correia for all his guidance and patience. Professor Luís gave me the chance to freely explore through a number of research options, without ever feeling anything but utmost support from him.

Second, I would like to thank Dr. Rob Mills who gave up his time to provide several contributions and insights into many aspects of this thesis. I owe Dr. Mills my gratitude for that.

A special thanks to all my fellows from the Cognitive Science Program. Particular acknowledgements to Marco Nunes, Bruno Penha and Rafael Nascimento for providing me with stimulant discussions and companionship.

To my childhood friends, for showing me that besides a world to understand there is a life to live.

Last but not least, I have to thank my family, without their unconditional and unwavering support I would have never achieved my goals in life. I owe my future success and happiness to you all, you mean everything to me. To my Mother, Father, Grandmother Maria, Grandfather Zé and sweet Pipinhas, the biggest thank you of all. I will always love you.

Resumo

Na presente dissertação, investigamos de forma sistemática a forma como a morfologia dendrítica subjaz as diferenças na atividade elétrica neuronal que estão na base da geração de potenciais de ação. De forma a atingir este objetivo desenvolvemos uma medida que quantifica as duas maiores fontes de variabilidade morfológica: métrica e topologia, e ainda outros componentes estruturais como canais iónicos. Baseado na nova medida, propomos um novo mecanismo de sincronização que relaciona a estrutura dendritica à modulação de currente axial que flui da árvore dendrítica até ao soma. Esta hipótese afirma que quanto mais simétrica a estrutura electrotónica da célula é, mais currente irá chegar ao soma das dendrites devido à sincronização obtida em virtude da simetria estrutural.

De forma a testar a hipótese de sincronização foram simuladas duas experiências usando modelos multi-compartimentais computacionais de células de Purkinje, Piramidais e células do córtex Visual. Na primeira abordagem, as estruturas das células foram quantificadas utilizando a nova medida e depois comparadas com a quantidade de currente axial proviniente das dendrites que atingia o soma. Na segunda abordagem, os potenciais de voltagem são medidos ao nível do compartimento axo-somático de forma a se poder analisar se diferenças encontradas na condição axial induzem diferenças na atividade de *spiking* da célula. Os resultados apoiam a hipótese de sincronização, pois neurónios com estruturas electrotónicas com níveis de simetria mais elevados, exibem os níveis mais elevados de currente axial a chegar ao soma para o mesmo estímulo. As diferenças encontradas na condição axial correlacionaram-se com o tempo que os neurónios levaram a atingir um potencial de ação, com os neurónios mais simétricos a requerer menos tempo para o fazer. No entanto, diferenças significativas não emergiram nos padrões de potenciais de ação, mas estes resultados podem ser explicados por algumas limitações no protocolo de estimulação. Em suma, os nossos resultados mostram que a medida desenvolvida é uma alternativa promissora às abordagens morfométricas tradicionais, pois pode ser utilizada com confiança para quantificar diferenças estruturais, podendo ser aplicada a vários tipos de neurónios, providenciando uma ligação entre estrutura e função.

***Palavras-chaves*: Estrutura-Função, Simetria, Estrutura Electrotónica, Sincronização**

Abstract

In this dissertation, we systematically investigate how dendritic morphology underlies the differences in the electrical dynamics of the cell that lead to spiking behaviour. To accomplish this goal we develop a new measure that provides a quantitative account of the two most relevant sources of morphological variability: metrics and topology, as well as of other structural components such as ion channels. Supported by the new measure, we propose a new synchronization mechanism that relates dendritic structure to the modulation of axial current that flows from the dendrites to the soma. This hypothesis states that the more symmetric the electrotonic structure of a cell is, the more current will reach the soma from the dendrites due to the synchronism obtained by virtue of structural symmetry.

To test the synchronization hypothesis two simulation-based experiments using detailed multi-compartmental computational models of Purkinje, Pyramidal and Visual cortical cells were conducted. In the first approach, by means of the novel measure, the structure of the cells are quantified, and compared with the amount of axial current reaching the soma from the dendritic tree. In the second approach, voltage traces are measured at the axo-somatic compartment to analyse whether differences found in the axial current condition induce differences in the output spiking patterns. Our results support the synchronization hypothesis, as neurons with electrotonic structures with higher levels of symmetry exhibited the highest amount of current reaching the soma for the same stimulus. These differences correlated with the time that neurons required to spike, with more symmetrical neurons requiring less time to do so. Nevertheless, significant differences fail to emerge in the output spike trains, but these results can be explained by some limitations in the stimulation protocol. Overall, the results show that the proposed measure is a promising alternative to traditional morphometrics measures as it can be used with confidence to quantify structural differences, and can be applied across different types of neurons while providing a bridge between structure and function.

Keywords: **Shape-Function, Symmetry, Electrotonic Structure, Synchronization**

Contents

List of Figures

List of Tables

List of Symbols

Symbol	Units	Description
d	μm	Diameter of the neurite
l	μm	Length of the compartment
R_m	Ωcm^2	Specific membrane resistance
R_{in}	Ωcm^2	Specific input resistance
C_m	μFcm^{-2}	Specific membrane capacitance
R_a	Ωcm	Specific axial resistance
r_m	Ωcm	Membrane resistance per inverse unit length
c_m	μFcm^{-1}	Membrane capacitance per unit length
r_a	$\Omega/$cm^{-1}	Axial resistance per unit length
V	mV	Membrane Potencial
E_m	mV	Leakage reversal potential due to different ions
I	μAcm^{-2}	Membrane current density
I_e	nA	Injected current density
I_c	nA	Capacitive current
I_i	nA	Ionic current
f	Hz	Frequency
Δt	μs	Time-step of the numerical integration
nseg		Number of compartments of a given neurite
Na^+		Sodium ion
Ca^{++}		Calcium ion
K^+		Potassium ion
d_λ		d_λ rule
τ_m	msec	Membrane time constant
λ	μm	Space constant
$\bar{g}_{leak}$	pS μm^{-2}	Membrane maximum leakage density
$\bar{g}_{Na}$	pS μm^{-2}	Fast sodium maximum conductance density
$\bar{g}_{Km}$	pS μm^{-2}	Slow voltage-dependent non-inactivating potassium current maximum conductance density

$\bar{g}_{Kv}$	pS μm^{-2}	Fast non-inactivating potassium current maximum conductance density
$\bar{g}_{Kca}$	pS μm^{-2}	Slow calcium- activated potassium current maximum conductance density
$\bar{g}_{Ca}$	pS μm^{-2}	High voltage-activated calcium current maximum conductance density
d_{syn}	pS μm^{-2}	Synaptic maximum conductance density
Temp	°C	Temperature

Chapter 1

Introduction

In this first chapter, we start by putting the present work into a bigger perspective and enumerate the main objectives of the research presented in the following manuscript. In the final section of the chapter, we provide an overview of the thesis structure.

1.1 Context

The shape–function paradigm, i.e., the existence of a close link between shape and function in nature, probably takes origin along with the beginning of human scientific thinking. This paradigm finds an excellent field of application in Neuroscience in a branch named Neuromorphology. This field yields not only the application of a set of techniques useful to measure and characterize the geometrical properties of nerve cells and structures, but more extensively cares about studying the relationship between the geometry of the nervous structure and its functionality [8]. In particular, this thesis is on the subject of how the structural features of single neurons may influences the electrical activity of the cell and its firing behaviour .

However, the task of relating structure to function is not an easy one because the brain is a extraordinarily complicated circuit. To make things more complicated the components of this circuit are not homogeneous, but instead, there are many different classes of neurons [15]. To fully understand the function of any circuit both the components and the connections must be identified and understood, but this is an extremely difficult task when considering the number of neurons in the brain [60].

Nevertheless, experimental and theoretical observations disclose many structural and functional patterns, leading one to think that must be underlying organizational principles that govern brain structure and allow the network to function [24].

Fundamental Research

One of the central questions in neuroscience is how particular tasks, or computations, are implemented by neural networks to generate behaviour. The prevailing view has been that information processing in neural networks results primarily from the properties of

synapses and the connectivity of neurons within the network, with the intrinsic excitability of single neurons playing a lesser role [69]. As a consequence, the contribution of single neurons to computation in the brain has long been underestimated .

However, in recent years, the role of neurons in these computations has evolved conceptually from that of a simple integrator of synaptic inputs until a threshold is reached and an output pulse is initiated [73], to a much more sophisticated processor with mixed analog-digital logic and highly adaptive synaptic elements [37, 59].

During this conceptual transition, it was realised that the morphology of a neuron, notably its dendrites, play a critical role in brain function for two main reasons [59]. First, neuronal morphology defines and is defined by the circuitry, being the synaptic contact between the output axon of one neuron and the input dendrite of another the major element of neuronal connectivity. As such, a precise morphology is crucial to establish the connectivity required for the nervous system to operate normally. Secondly, the precise morphology of a neuron and its membrane's ion channel composition set the computations that a neuron performs on its inputs, i.e., the propagation and integration of synaptic input signals along the neuron's membrane up to the axon initial segment, the location where the neuronal output is typically generated. Therefore, it has been hypothesised and demonstrated in some cases that neurons with different structures serve different functions or endow different computational capabilities [24].

In spite of it is nowadays a given fact the existence of a link between structure and function, the mechanisms underlying this link are poorly understood, and consequently the impact of morphological differences on the cell behaviour remains insufficiently known [69, 88]. This situation is a consequence of the complexity of single neurons: these cells have many branches with irregularly varying diameters and lengths, their membranes are populated with a wide assortment of ionic channels that have different ionic specificities, and kinetics dependent on voltage and second messengers. Trying to incorporate every of these biological details may obscure the focus on the essential structure-function relation, whereas limiting investigations to highly abstract processes may reduce the biological relevance of specific findings.

Moreover, scattered over the surface of the cell may be hundreds or thousands of synapses, and synapses themselves are far from simple, often displaying stochastic and use-dependent phenomena that can be quite prominent, and frequently being subject to various pre and postsynaptic modulatory effects. In sum, even a single isolated neuron is an intricate world on its own [49].

Despite this daunting complexity, even if the brain was perfectly static, it seems unlikely that the genome could encode the location of every synapse and therefore the location of every piece of a dendritic tree and axon from every neuron. It seems probable that the genome specifies general rules, mechanisms or strategies for connectivity and structure, and then connections form within the context of these general rules [8]. The long-term end result of the collective effort by researchers in Computational Neuroscience at large is

to identify these general rules and build a comprehensive structural and functional model of the brain [72]. Such a model might have deep implications for scientific understanding as well as technological development.

Translational Research

The unravelling of these general rules not only has importance for fundamental purposes but also has many possible important applications at different levels. For example, various studies report that many neuropsychiatric disorders are characterized by dendritic and synaptic pathology, including abnormal spine density and morphology, synapse loss, and aberrant synaptic signaling and plasticity [57, 66, 93]. Therefore, identifying and understanding these changes in neuronal morphology are essential for understanding brain function in normal and disease states.

Moreover, theories and methods of bio-inspired Artificial Intelligence, such as Neural Engineering, aim at reproducing the functionalities of brains in order to engineer intelligent machines. Issues addressed by Neural Engineering that Computational Neuroscience may help shed a light on include high-level architectures that could reproduce cognitive abilities, brain-computer interfaces and implementation of neural models in hardware [34, 46, 50].

1.2 Research Objectives

Taking into account what was previously mentioned, the scientific issue that motivates the design and construction of the models analysed in the present thesis, is the question of how signal integration is affected by the structure and biophysical properties of neurons. Especially, the objectives of the present manuscript are:

- Systematically investigate how the physical parameters controlled by dendritic morphology underlies the differences in the electrical dynamics of the cell that leads to spiking behaviour.

- The developed approach should provide a quantitative account of the two sources of morphological variability: metrics (size of the dendritic tree, segment lengths, segment diameters) and topology (the way the segments of the dendritic tree are connected) and possibly of others structural components such as ion channels.

- Since there are not any such measures in the literature, one of the main goals of the research conducted was to create a measure as general as possible, i.e., that could be applied across many types of neurons.

1.3 Research Contributions

The work developed in this thesis comprises the following contributions:

- This thesis is the first to introduce in the Computational Neuroscience domain a measure, e^{-X}, that quantifies topological, metrical, passive and active properties of neurons in a unified way.
- Our results show that e^{-X} has a highly discriminative power, and it provides a direct bridge between structure and function. We compare e^{-X} to other more traditional approaches.
- Based on the novel measure it is proposed a new structure based mechanism that neurons may explore to integrate electrical signals. We hypothesised how symmetric electrotonic dendritic structures lead to better electrical signals synchronization.
- Using computational models of artificial reconstructed neurons, we manipulate the dendritic mechanism to determine if there is a causal link between the proposed mechanism and the electrical behaviour of the cells. Our simulation-based experiments show that the proposed mechanism is a robust and important factor modulating axial current that causes neurons to spike.

1.4 Report Overview

In this section, we provide an overview of the thesis structure. In Chapter 2, we review the state-of-the-art on the distinct subjects relevant to this dissertation. The chapter is divided into three main sections that are dedicated respectively to the computational approach in Neuroscience, the role of single neurons in information processing, and to the realistic modelling of single neurons.

In chapter 3, we discuss the morphological features of dendritic tree structures, providing an overview of quantitative procedures used to accomplish that. The main focus of the chapter is on the description of morphological complexity of neurons and how one can use this description to unravel neuronal function in dendritic trees and possibly in neural circuits.

In chapter 4, we describe and discuss some advanced preliminaries, necessary in order to understand the theoretical part of the research presented. Basically, we derive and introduce a new measure that relates structure to function in single neurons, and in the end of the chapter the research problem is stated.

In chapter 5, it is provided a description of the approach and method employed to solve the stated problem, and in the final section of the chapter the results found are analysed and discussed.

In chapter 6, the work done in the present thesis is positioned in the context of other people's efforts in the area. It is shown the principal differences and similarities with respect to the details of the problem, the approach, the results, and the methodology. Then we discuss directions for future work. Finally, we give a summary of the report and present some conclusions.

Chapter 2

Background

This chapter includes a broad range of subjects relevant to this dissertation. The subjects are presented in a top-down fashion. First, we are going to expose the reader to the field of Computational Neuroscience, particularly to its advantages and disadvantages, and how Neuroscience as a whole can benefit from this approach. Afterwards, we are going to review the state of the art of single neuron computational abilities, this means how they process information in order to execute certain tasks, providing theoretical and experimental examples to support. In the final section of the present chapter, we will introduce the techniques used to implement morphologically realistic models of single neurons.

2.1 The Computational Approach

The use of computational tools to Neuroscience is known by a number of largely synonymous names, such as Computational Neuroscience, Theoretical Neuroscience or Computational Neurobiology. This field has a twofold approach: in one hand, it comprehends the use of databases, the World Wide Web, visualization of data, storage and analysis of Neuroscience data [6, 22, 78]. On the other hand, it attempts to analyse computational models of the nervous system by using powerful computers to find numerical solutions to the complex sets of equations needed to construct an appropriate model of certain parts of the nervous system [16, 20, 38].

2.1.1 What is a Computational Model?

The complexity of the nervous system makes it very difficult to someone to theorise about it, in a convincing manner, on how such system is put together and how it functions. To aid our thought processes we can represent our theory as a computational model in the form of a set of mathematical equations. The variables of the equations represent specific neurobiological quantities, such as the rate at which impulses are propagated along an axon, or the frequency of opening of a specific type of ion channel, and the equations

themselves represent how these quantities interact according to the theory being expressed in the model [16, 20, 37, 41].

Advantages

A key advantage of computer modelling is its ability to wrestle with complexity that often proves daunting to otherwise unaided human understanding, and because of this, the use of computer models to understand how the brain works has been a critical contributor to scientific progress in this area over the past few years. Solving these equations by analytical or simulation techniques enables us to show the behaviour of the model under given circumstances, and thus address the questions that a certain theory was designed to answer [16, 20]. By doing so, these models can be used as explanatory or predictive tools, removing ambiguity from theories and complement empirical experiments (sometimes some computational models can even explore conditions that are very difficult to test empirically).

Disadvantages

Nevertheless, in all fields where computer models are used, there is a fundamental distrust of these models. They are themselves complex, created by people, and have no necessary relationship to the real system in question.

A key aspect of computational modelling is determining values for model parameters and often these will be estimates at best, or even complete guesses. To avoid this drawback, a good model must be constrained by empirical data at as many levels as possible, and they must generate predictions that can then be tested empirically [41].

Another known issue in computational modelling in general, and in computational modelling applied to Neuroscience in particular, is the trade off between incorporating sufficient details to account for biological complexity, and reducing this complexity to a bare minimum to make the model tractable [49]. The nature of the scientific question that drives the modelling work will largely determine the level at which the model is to be constructed, and therefore the level of details to be incorporated, but the general rue of thumb is to develop the simplest possible model that captures the most possible data. Often this is a matter of judgement on what phenomena someone regards as being important, and once again, this will vary depending on the scientific questions being addressed with the model.

2.1.2 Developing a Computational Model

To develop a computational model in neuroscience the researcher has to decide how to construct and apply a model that will link the neurobiological reality with a more abstract formulation that is analytical or computationally tractable. As previously mentioned, guided by neurobiological data, decisions have to be made about the level at which the

model should be constructed, the nature and properties of the elements in the model and their number, and the ways in which these elements interact. Having done all this, the performance of the model has to be assessed in the context of the scientific question being addressed.

Conceptual Model

The first step is to formulate a conceptual model that attempts to capture just the essential features that underlie a particular function or property of the physical system. If the aim of modelling is to provide insight, then formulating the conceptual model necessarily involves simplification and abstraction [16, 20, 41].

When we formalize our description of a biological system, the first language we use is Mathematics, by doing so one specify the theory in a non-ambiguous and precise way. The conceptual model is usually expressed in mathematical form, although there are occasions when it is more convenient to express the concept in the form of a computer algorithm.

Section 2.2.3 is concerned with mathematical and conceptual representations of phenomena relevant to model single neurons.

Computational Model

A computational model is a working embodiment of a conceptual model through the medium of computer simulation [16, 20, 41]. It can assist hypothesis testing by serving as an artificial laboratory preparation in which the functional consequences of the hypothesis can be examined. The conceptual model, and the hypothesis behind it, determine what is included in the computational model and what is left out.

Such tests can be valid only if the computational model is as faithful to the conceptual model as possible. This means that the computational model must be implemented in a way that does not impose additional simplifications or introduce new properties that were not consciously chosen by the user. Otherwise the interpretation of the results obtained can become compromised, because they just might be a byproduct of distortions produced by trying to implement the model with a computer.

Section 2.3 of the present chapter will deal with the techniques used in the constructions of morphologically realistic models of single neurons.

2.2 The Single Neuron

The fundamental building block of every nervous system is the single neuron. Understanding how these sophisticated elements operate is an integral part of the quest to solve the mysteries of the brain. An important contemporary concept of the neuron doctrine is that the neuron is made of several regions with different functions interacting in complex ways

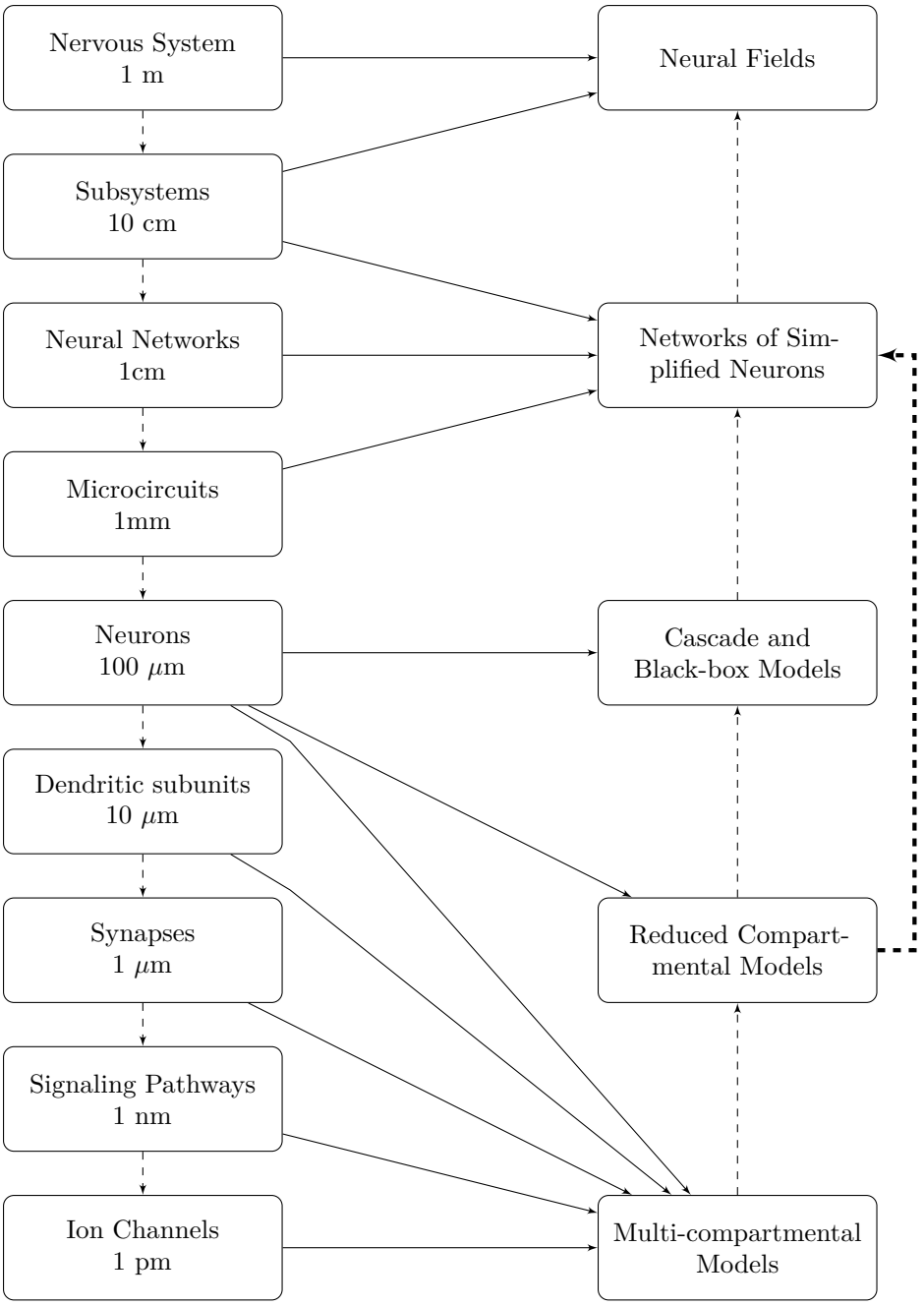

Figure 2.1: To fully comprehend the nervous system it is required to understand it at many different levels, at spatial scales ranging from metres to nanometres or smaller. At each of these levels there are different computational models for how the elements at that level function and interact. The appropriate level of description depends on the particular goal of the model. **Multi-compartmental Models**: morphologically realistic models that focus on how the spatial structure of a neuron contributes to its dynamics and function [49, 41]. **Reduced Compartmental Models**: these models offer a good compromise between realism and computational efficiency when studying single neurons [49, 41]. **Cascade and Black-Box Models**: these models are the highest level models for single neuron modelling, and basically they are simplified functional models of neural spike responses [49]. **Neural Networks of Simplified Neurons**: interconnected sets of reduced compartmental neurons that simulate the function of biological neural networks, such as synchronization and oscillations [37]. **Neural Fields**: are even higher level models of neural networks; the equations are tissue level models that describe the activity (i.e. pattern formation) of large chunks of neurons populations [37].

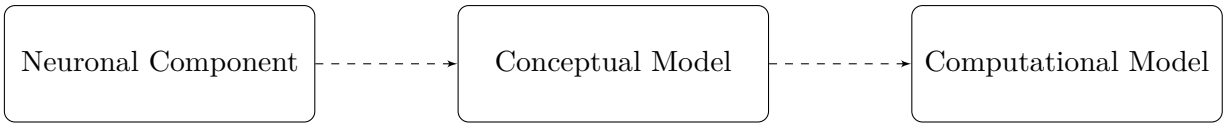

Figure 2.2: Creating a computational model of neuronal component/phenomena involves two steps. The first step deliberately omits real-world complexities to produce a **conceptual model**. In the second step, this conceptual model must be faithfully translated into a **computational model** [20].

and these functionally diverse regions correspond to anatomically distinct parts of the cell [56].

The *axon* is a component of a neuron specialized to distribute or conduct nerve impulses generally over great distances. It is smooth and only sends off branches at long intervals, if at all. It is commonly surrounded by a barrier of non-nervous cells called *neuroglia* inside the central nervous system, and *schwann cells* outside (see Figure 2.3).

The *dendrites* are tree-like structures specialized for collecting information from other neurons, neuroglia, circulating hormones and extracellular signals to the cell body or *soma*. Vertebrate dendrites are commonly highly branched, irregular in thickness, thorny and are covered by cocktail of excitable channel types. The neuronal cell membrane, explores its permeability to different ions and concentration gradients across the membrane to perform complex manipulations of signals representing internal and external worlds.

In the following subsections, we will provide an overview of Cable Theory applied to model the spread and propagation of voltage and currents in neurons. This approach started with Wilfrid Rall's seminal contributions in the sixties [83]. Particularly, the equations that are going to be presented in the following pages constitute the base of the multi-compartmental models used later in this thesis.

2.2.1 Dendritic Integration

The input-output relation in neurons can be studied in two opposing points of views: **neural encoding** and **neural decoding** [27]. On one hand, neural encoding refers to the study of how neurons respond/integrates a particular stimulus, and the construction of models that attempt to predict the response to those stimuli. This is the topic of the present subsection.

In the other hand, neural decoding is concern with analysing the amount of information encoded by sequences of action potentials. This issue will be briefly exposed in the following subsection 2.2.2.

A typical neuron receives inputs from thousands of other neurons through the contacts on its synapses (see Figure 2.3), and dendrites receive the far majority of these synaptic inputs [56]. The inputs produce electrical transmembrane currents that change the membrane potential of the neuron. Synaptic currents produce changes, called postsynaptic

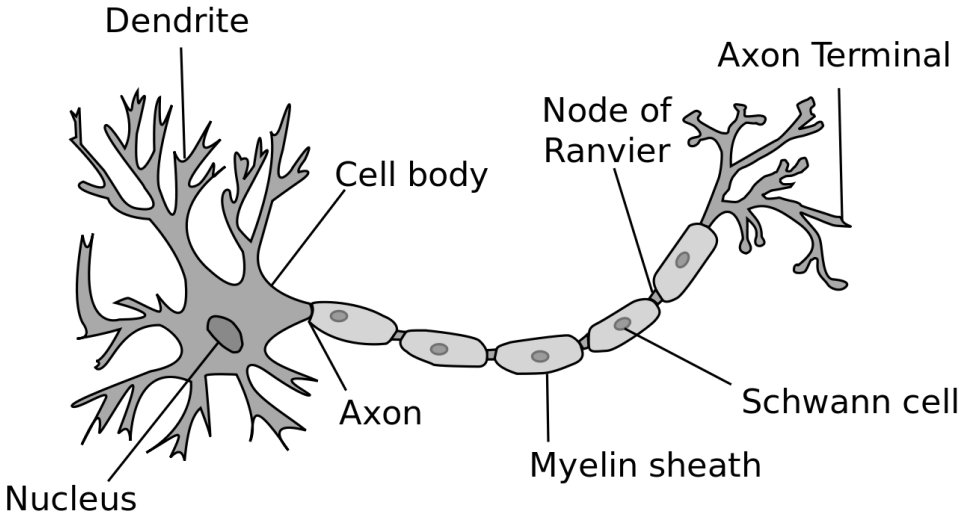

Figure 2.3: The **axon terminal buttons** are the connection points between sending neurons (**pre-synaptic**) and the **synapses** of receiving neurons (**post-synaptic**). Most synapses are on **dendrites**, which is where the neuron integrates all the input signals. Then, all these signals flow into the main dendritic trunk and into the cell body or **soma**, where the final integration of the signal takes place. The thresholding takes place at the start of the axon, named **axon hillock**. The **axon** also branches widely and is what forms the other side of the synapses onto other neuron's dendrites, completing the next chain of communication [56].

potentials (PSPs). Small currents produce small PSPs; larger currents produce significant PSPs that can be amplified by the voltage-sensitive channels embedded in the neuronal membrane and lead to the generation of an *action potential* or *spike* – an abrupt and transient change of membrane voltage that propagates to other neurons via the axon [56].

In an active neuron the superposition of passive and active electrical properties serves to allow the cell the possibility of summing the transmembrane potential either linearly or nonlinearly and to reach depolarization levels sufficiently high to trigger action potentials [84].

Passive Properties

Even though it is rare to find fully passive dendrites in the mammalian brain, i.e., that do not contain voltage-dependent membrane conductance, it is important to recognize that the passive properties of the dendritic tree provide the backbone for the electrical signalling in dendrites, and enhance the computational power of neurons, making understanding the passive properties of dendritic trees crucial for the fully comprehension of the single neuron computations [60, 83].

In terms of signal propagation, dendrites behave like electrical cables with medium-quality insulation, and this propagation depends on R_m and C_m that may vary from cell to cell [60, 84]. As such, passive dendrites linearly filter the input signal as it spreads to the soma, where it is compared with the threshold. This filtering tends to attenuate and temporally delay the dendritic signal as a function of the distance it travels and the frequency of the original signal. Thus a brief and sharp excitatory postsynaptic potential

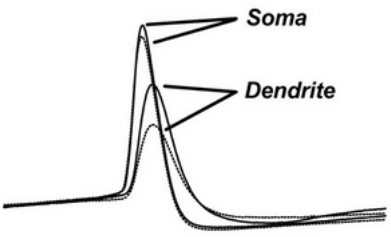

Figure 2.4: Voltage traces of EPSP recorded ate the soma, from synapses located away from the soma and close to the soma. Passive dendrites function as a low-pass filter and slows the time course as measured at soma, thus increasing temporal summations at the soma.

(EPSP) that originates in the dendritic tree will be transformed into a much smaller and broader signal when it arrives at the soma. Nevertheless, these factors are not the only factors that influence the PSPs propagation in a dendritic tree. The geometry of the dendritic tree, coupled with a unique synaptic architecture, influences signal propagation as well and may implement specific computations [45, 84].

Synaptic events are conductance changes, rather than voltage sources, and their interaction is significantly constrained by dendritic morphology. **Spatial summation** describes the interaction of coincident synaptic inputs and depends on their relative locations within the dendritic tree, and **temporal summation** describes the interaction of coincident synaptic inputs and depends on their relative offset and time course (which itself depends on $\tau_m = R_m * C_m$) [84]. One important result regarding these two types of summation is that sublinear summation is expected for synapses located close together (or temporally correlated), but it is minimal, or non existent for spatially (temporal) separated inputs. However, this sublinear summation is modulated by interactions between spatial and temporal summation, with summation reaching almost linear additivity when a certain balanced is reached between the two. For example, if two synapses are contiguous spatially, the summation is maximum when a certain amount of temporal delay between the onset of both happens, and vice-versa, until a limit is reached and the two synapses do not interact electrically. This happens because the depolarization caused by one synaptic event reduces the driving force at nearby synaptic locations [45]. These principles governing dendritic integration of EPSPs apply similarly to IPSPs (inhibitory postsynatic potentials).

Taking into account the principles stated, and the interaction between excitatory and inhibitory PSPs, it is obvious that with certain synaptic arrangements in a passive dendritic tree alone, nonlinear computations can be implemented (see Figure 2.5 as an example).

Active Properties

Many types of neurons display voltage-dependent membrane conductances in their dendrites. The presence of these active conductances in dendrites has important consequences for synaptic events and their integration. Depending on their voltage dependence, ionic specificity, and kinetics, dendritically expressed voltage-gated channels have the poten-

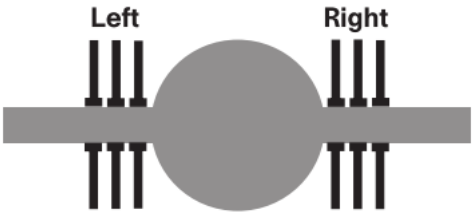

Figure 2.5: Neuron model that mimics the algorithm implemented by auditory neurons. The model consists of a soma (centre) and two cylindrical dendrites. The task of a brainstem auditory neuron is to perform coincidence detection in the sound localization system, i.e. it has only to respond if the inputs arriving from both ears coincide in a precise manner, while avoiding a response when the input comes from only one ear. Inputs to each ear do not produce strong enough PSPs, but the input from both ears is summed and compared with threshold, and this sum exceeds the threshold, whereas if the input arrives only to one ear the output is not large enough. Agmon-Snir et al. [1] showed that dendrites of these neurons might implement a similar algorithm. This is an example of how the dendritic tree geometry, coupled with a unique synaptic architecture, implements specific computations that are beneficial for single neurons computations. (This picture was taken from [1])

tial to amplify, dampen, and shape synaptic responses as they propagate through the dendritic tree, expanding the computational repertoire of a neuron [59, 60, 69]. While a comprehensive discussion of all dendritically expressed channels is beyond the scope of this review, several dendritic conductances stand out at being especially important for synaptic integration across a wide range of neurons, such as:

- active dendrites can influence the integration of PSPs is by amplification of inputs, because the fact that passive dendrites attenuate the synaptic input. There have been proposed several mechanisms, all off them with experimental support, for this, namely *sypnatic scaling*, *subthreshold boosting*, *local dendritic spikes*, *global dendritc spikes* [69, 21].

- interactions between voltage-dependent conductances can also underlie the generation of intrinsic subthreshold oscillations, which have been demonstrated in various cell types (e.g. place fields in hippocampus [3]).

- strong local dendritic nonlinearities, caused by the presence of voltage-gated and calcium channels, may transform a dendritic tree in a set of multiple subunits, such as single dendritic branches, that independently process input and convey the signal to the soma through an amplitude boosting nonlinearity [35, 69].

Besides the information just stated, there are many other ways in which voltage-dependent conductances can shape membrane-potential dynamics and neural computation that we have not reviewed here.

Computation	Biophysical Mechanism
Addition or subtraction	Dendritic summation of excitatory and/or inhibitory inputs
Subtration	Shunting inhibition plus integrate-and-fire mechanism
Multiplication or division	Synaptic interaction Gain modulation via synaptic background noise
High-pass filter	Firing rate adaption
Low-pass filter	Passive membrane properties
Toggle switch	Bistable spike generation

Table 2.1: Basic computations that follow from generic neuronal properties. These simple computations can be used together in the same neuron to create algorithms that process the information in a behavioural relevant way, e.g. collision avoidance, sound localization, motion detection [49].

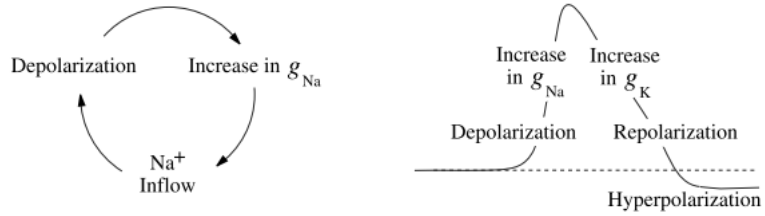

Figure 2.6: Action potentials are generated and sustained by ionic currents through the cell membrane. The ions most involved are sodium, Na^+, and potassium, K^+. In the simplest case an increase in the membrane potential activates (opens) Na^+ (and/or Ca^{++} channels), resulting in rapid inflow of the ions and further increase in the membrane potential. Such positive feedback leads to sudden and abrupt growth of the potential. This triggers a relatively slower process of inactivation (closing) of the channels and/or activation of K^+ channels, which leads to increased K^+ current and eventually reduces the membrane potential. (This picture was taken from [51])

2.2.2 Spiking

Neurons are slow, unreliable analog units, yet working together they carry out highly sophisticated computations in cognition and control [77]. Action potentials play a crucial role among the many mechanisms for communication between neurons, and other physiological processes such as cell division, fertilization, morphogenesis, secretion of hormones, ion transfer and cell volume control [52]. They are abrupt changes in the electrical potential across a cell's membrane, and they can propagate in essentially constant shape away from the cell body along axons and toward synaptic connections with other cells (see figure 2.4).

Threshold

A lot of attention has been spent trying to experimentally determine the firing voltage thresholds of neurons, but unfortunately, no clear voltage value was found above which neurons fire. Instead it has been proposed, a new concept called *rheobase*, i.e., the minimal amplitude of injected current of infinite duration needed to fire a neuron.[51].

Having this concept in mind, neurons can be classified in terms of its excitability

into two great classes: **integrators** and **resonators** [51]. The first class has well defined thresholds, and if a certain amount of positive current reaches the soma there will be enough depolarization to induce an action potential, i.e., they integrate the signals; and the higher the frequency of the input, the sooner they fire.

On the other hand, the second class may not display a well defined threshold, instead they respond preferentially only to certain frequencies of the input, so the occurrence, or not, of spiking behaviour is dependent on the temporal characteristics of the stimulus.

Neural Code

Action potentials convey information through their timing. A chain of action potentials is called a *spike train*, i.e., a sequence of spikes events which occur at regular or irregular intervals. The analysis of how neurons communicate through spike trains is one of the greatest endeavours of modern Neuroscience, and it is named as the **neural code** [27].

Known coding strategies used by single neurons can be divided approximately into **rate codes** and **temporal codes**, but these terms have been used inconsistently and are prone to confusion [27]. In the former, the number of spikes within a time window correlates with some stimulus attribute, i.e., emphasis is put on average spiking activity. In the former, special importance is given to precise spiking time, being this precision used to encode information. It has been found that the this temporal resolution is on a millisecond time scale, indicating that precise spike timing is a significant element in neural activity [37].

In sum, variability is a prominent feature of neural activity and its sources and functional implications are the focus of much investigation [43]. Different patterns of spike trains place limits on the reliability of signals, but can also provide a rich language for neuronal populations and their interactions. This analyses of variability [43] it is out of the scope of this thesis, but it is important to focus on the fact that different temporal patterns of spike trains may have different neurocomputational properties, and cause different responses on the postsynaptic neuron [52, 53, 86].

2.2.3 Cable Theory

Neurons display a wide range of dendritic morphologies, ranging from compact arborizations to elaborate branching patterns. At the simplest level, the dendritic tree can be treated as a passive electrical medium that filters incoming synaptic stimuli in a diffusive manner. The current flow and potential changes along a branch of the tree may be described with a second-order, linear partial differential equation commonly known as the **cable equation** [9, 17, 32, 33, 37, 41, 60, 64][1].

Even though the derivation of the cables equations are out from the scope of this review, it is import to note that the cable equation is based on a number of approximations: *(i)*

[1] Any of these references provide excellent reviews to linear, and nonlinear cable theory, and serve as our basic references in the following subsection.

magnetic fields due to the movement of electric charge can be neglected; *(ii)* changes in ionic concentrations are sufficiently small so that Ohm's law holds; *(iii)* radial and angular components of voltage can be ignored so that the cable can be treated as one-dimensional medium, and *(iv)* for the linear case, dendritic membrane properties are voltage-independent (passive), that is, there are no active elements.

Linear Cable Equation

The basic equation governing the dynamics of the membrane potential in thin and elongated neuronal processes, such as axons or dendrites, is the cable equation. A nerve cable consists of a long thin, electrically conducting core surrounded by a thin membrane whose resistance to transmembrane current flow is much greater than that of either the internal core or the surrounding medium. Injected current can travel long distances along the dendritic core before a significant fraction leaks out across the highly resistive cell membrane. The cable equation[2] is a partial differential equation (PDE) with the form:

$$C_m \frac{\partial V}{\partial t} = \frac{E_m - V}{R_m} + \frac{d}{4R_a} \frac{\partial^2 V}{\partial x^2} + \frac{I_e}{\pi d} \tag{2.1}$$

In the cable equation the membrane potential is a function of distance x along a continuous cable, and time $V(x,t)$ and $I_e(x,t)$ is the current injected per unit length at position x.

Boundary Conditions

In Cable Theory, there are three boundary conditions with important physical significance: killed end, leaky end and sealed end.

The simplest case is that of a **killed end**, in which the end of the neurite has been cut, and it means that the intracellular and extracellular media are directly connected at the end of the neurite. Thus the membrane potential at the end of the neurite is equal to the extracellular potential. To model this, one specifies the value of $V = 0$ to one of the egdes of the cable.

If the end of the neurite is intact, a different boundary condition is required, named **selead end**. Here, because the membrane surface area at the tip of the neurite is very small, its resistance is very high. Since the axial current is proportional to the gradient of the membrane potential along the neurite, zero current flowing through the end implies that the gradient of the membrane potential at the end is zero.

It can also be assumed that there is a **leaky end**; in other words, that the resistance at the end of the cable has a finite absolute value. In this case, the boundary condition is derived by equating the axial current, which depends on the spatial gradient of the membrane potential, to the current flowing through the end.

[2]Please see list of symbols

Analytical Solutions

The cable equation can be solved analytically for these boundary conditions, i.e., one can find mathematical expressions for the time course of the membrane potential at different points along a passive cable in response to pulses of current or continuous input such as step current. Solving an equation analytically (in this case) means that an expression for how the membrane potential depends on position and time can be derived as a function of the various parameters of the system. Although modern computers can numerically integrate the equations with high resolution, looking at analytical solutions can give a deeper understanding of the behaviour of the system.

Several key concepts associated with the linear cable equation for a single finite or infinite cylinder are the **space constant** λ, determining the distance over which a steady-state potential in an infinite cylinder decays e-fold[3] , the neuronal **time constant** τ_m, determining the charging and decharging times of $V(x,t)$ in response to current steps, and the **input resistance** R_{in}, determining the amplitude of the voltage in response to slowly varying current injections.

The voltage in response to a current input, whether delivered by an electrode or by synapses, can be expressed by convolving the input with an appropriate Green's function. For passive cables, this always amounts to filtering the input by a low-pass filter function, what does add by itself an important nonlinearity to neurons, and consequently enrich their computational capabilities, as it was shown in many occasions [83].

Nonlinear Cable Equation

Given the widespread existence of different classes of ion channels, namely voltage-activated, calcium-activated ion channels, and transmitter-activated ion channels involved in synaptic transmission, a realistic model of a biological neuron has to account for these nonlinear elements. However, analysing the properties of linear (passive) cable is still important because one needs to study the concepts and limitations of linear cable theory before advancing to more complex nonlinear phenomena.

The inclusion of these nonlinear elements[4] leads to the generalization of equation (2.1) into the following PDE:

$$C_m \frac{\partial V}{\partial t} = -\sum_k I_{i,k}(x) + \frac{d}{4R_a}\frac{\partial^2 V}{\partial x^2} + \frac{I_e(x)}{\pi d} \tag{2.2}$$

Basically, at any point in the neuron, the sum of axial currents flowing into the point is equal to the sum of the capacitive, ionic and electrode transmembrane currents at that point.

Nevertheless, we have seen that analytical solutions can be given for the voltage along a passive cable with uniform geometrical and electrical properties, but unfortunately, the

[3]This is the parameter controlling the voltage decay on classical electrotonic distance reviewed on section 4.3

[4]Ion channels can exhibit complex dynamics that is in itself governed by a system of differential equations.

same approach will not work because the formalism based on Green's functions cannot be applied to the previous equation, and therefore no analytical solutions can be found. So, the behaviour of the different kinds of nonlinear cable equations that may be created are better studied using numerical simulation methods, or by analysing the phase plane of the equation(s).

2.3 Multi-compartmental Models

As we see in section 2.2.1, the cable equation can be solved analytically only for simple cases, because even if the active conductances formed by nonlinear ion channels were neglected, a dendritic tree is at most locally equivalent to a uniform cable. Numerous bifurcations and variations in diameter and electrical properties make it really hard to find a solution analytically.

2.3.1 Spatial Discretization

When the complexities of real membrane conductances are included, the membrane potential must be computed numerically. This is done by splitting the neuron being modelled into separate compartments, and approximating the continuous membrane potential $V(x,t)$ by a discrete set of values representing the potential within the different compartments. This approach assumes that each compartment is small enough so that there is negligible variation of the membrane potential across it. In sum, the branched architecture typical of most neurons is dealt with by combining different cable equations, with appropriate boundary conditions in one big system of PDE's and solve it numerically [16, 20, 41].

In a multi-compartment model, each compartment satisfies an equation similar to equation (2.2), but the compartments are coupled to their neighbours. The following equation determines how the voltage V_j in compartment j changes through time:

$$C_m \frac{dV_j}{dt} = -\sum_k I_{i,k,j} + \frac{d}{4R_a}\frac{V_{j+1} - V_j}{l^2} + \frac{d}{4R_a}\frac{V_{j-1} - V_j}{l^2} + \frac{I_{e,j}}{\pi dl} \tag{2.3}$$

where $j+1$ and $j-1$ are the adjoining compartments. When the compartments is at a branching point, instead of just two adjoining compartments there will three, and since, there are no data for the systematic occurrence of trifurcations in dendritic trees, this will be the highest possible number of adjoining compartments.

The single biggest problem with constructing a compartmental model is to choose at what resolution capture the actual morphology of the real neuron being modelled. In one hand, increasing morphological accuracy means better approximation of the real system, but the other hand, more compartments and greater model complexity.

After the morphology has been compartmentalised, those compartments must be divided into electrical compartments. The choice of compartment size is an important

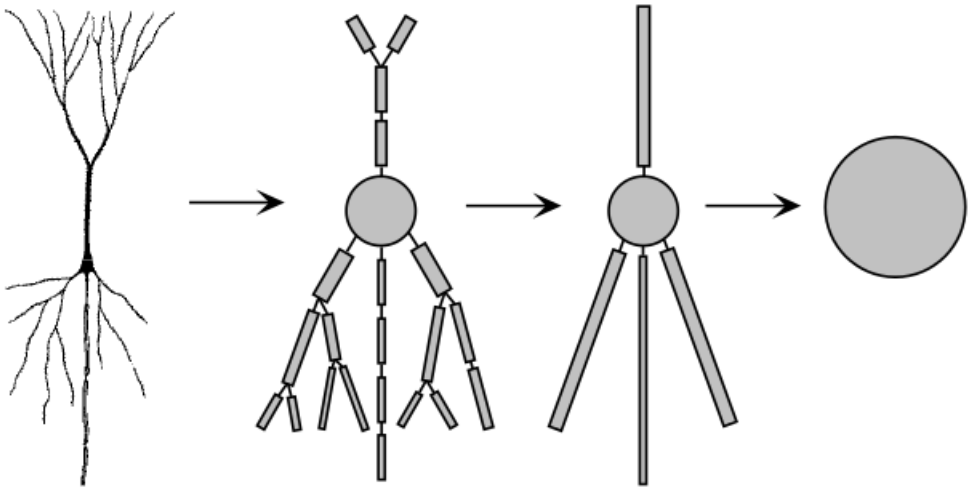

Figure 2.7: From left to right, biological neuron, multi-compartmental model, reduced compartmental model, single compartment model. The general approach in multi-compartmental modelling is to represent parts of the dendritic tree, soma and axon as quasi-isopotential sections with simple geometric forms, such as spheres or cylinders. This allows easy calculation of compartment surface areas and cross-sectional areas, which are needed for calculation of current flow through the membrane and between compartments. The bigger the number of compartments in a model is, the better is the accuracy of that model (this picture was taken from [27]).

parameter in the model and the output of because is required a good balance between accuracy and computational efficiency. There are several rules that can be used but the one used in the models designed in the present thesis is the d_λ rule [20]. Basically, an electrical compartment can not have a size bigger than 10% of λf, where λf:

$$\lambda f = \frac{1}{2}\sqrt{\frac{d}{\pi f R_a C_m}} \tag{2.4}$$

and f is set to be betweeen 50-100 Hz. Nevertheless, the choice depends on the desired spatial accuracy needed for the particular situation to be simulated. If one needs to know the value of a parameter, such as axial current, that varies over the cell morphology, to a specific spatial accuracy, then we must design a model with a sufficient number of compartments to meet that accuracy.

2.3.2 Temporal discretization

After the spatial discretization one has a large system of ordinary differential equations for the membrane potential at the chosen discretization points as a function of time. This system of ordinary differential equations has to be treated by numerical integration methods, i.e., algebraic expressions that approximate the differential equations are derived and by doing so it allows the calculation of quantities at specific predefined points in time [16, 20, 41].

Moreover, neurons are distributed analog systems that are continuous in space and time, but digital computation is inherently discrete. Because of this fundamental disparity,

implementing a model of a neuron with a digital computer raises too many purely numerical issues that have no relationship to the biological questions that are of primary interest, yet must be addressed if simulations are to be tractable and produce reliable results.

There are several numerical integration methods, and the use of a particular set of these methods may vary from simulator to simulator. The discussion of these methods is out of the scope of this thesis, but NEURON software [20], the package used to create and simulate the models present in the this thesis, makes available the following integration methods: backward Euler method, Crank-Nicholson, CVode, and DASPK. The choice between different methods is readily accessible for the users of the package, but the best way to determine which is the method of choice for a particular problem is to run comparison simulations while using these different methods, and different time-steps (Δt).

2.4 Summary

In this chapter, we introduced the field of Computational Neuroscience, particularly the topic of single neurons computations. First, we start by introducing some conceptual concerns of this field, and then we move to explain some of the single neurons computation properties. Afterwards, there was exposed how to model neurons as physical systems with Cable theory and Compartmental models.

Chapter 3

The Shape-Function Paradigm

This chapter focus on the morphological features of neuronal structure, particularly dendritic trees structure. We provide an overview of quantitative procedures for data collection, analysis, and modelling of dendrite shape. Our main focus lies on the description of morphological complexity and how one can use this description to unravel neuronal function in dendritic trees and neural circuits.

3.1 Dendritic Shape Paradigms

The shapes of the dendritic arborization of neurons is a unique property which differentiates the nervous tissue from all the other tissues of the organism. Over fifty years ago, Ramón y Cajal observed a great number of neurons stained with the Golgi method in a variety of species. The comparison of dendritic morphologies of neurons located in homologous regions of the brains of different animals led him to formulate what is called the **shape hypothesis**.

In a broader perspective, the shape hypothesis is a concept within other principles operating in evolution. The evolution of progressively more complex functions has been made possible by the evolution of more complex structural patterns, hence more complex connectivity and greater differences between individual neurons. From lower to higher animals there is a scale of increasing complexity in connectivity patterns that is made possible by greater structural specificity and resolution in the morphogenetic mechanisms by which neurons become a highly complex system. How neurons grow into the fantastic patterns of connections that bring about their properties, which make in turn their richness of behaviours, remains unknown. We know that the driving forces of evolution have created the conditions for an enormous increase in the number of elements,and this structural complexity is the background that provides for complex manipulations of signals representing internal and external worlds [85].

In the shape-function paradigm, there have appeared two not opposing views which try to explain the structural diversity found in the dendritic trees. These two views differ on the emphasis they put on which factors influence the most the shape of dendritic trees.

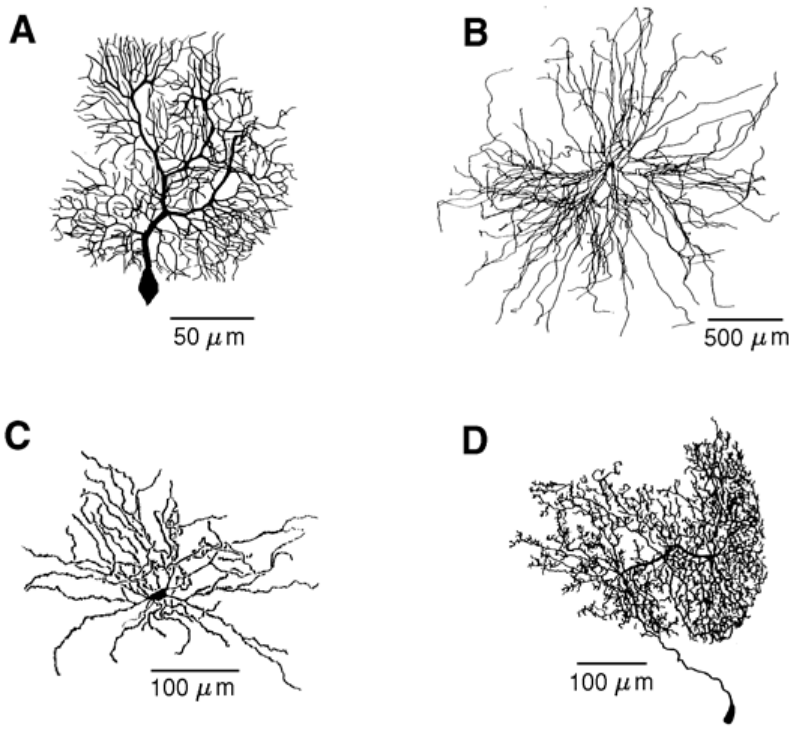

Figure 3.1: Different dendritic morphologies are present through neural systems. (**A**) Cereberall Purkinje cell, (**B**) α motorneuron, (**C**) Neostriatal spiny neuron, and (**D**) Interneuron.

On one hand, we find the **computational paradigm** where the emphasis is put on how the dendritic structural differences, coupled with synapses and ion channels, may enable the implementation of different computations that influences the firing output [8, 24]. On the other hand, we find the **wiring optimization paradigm**, and in this framework dendritic shape in particular, and the brain in general, are seen as a huge optimization problem. Basically, dendrites are a mean to maximize a neuron connections to to other neurons, while keeping wiring length and volume to a minimum, while taking into account metabolic constraints [12, 26, 80].

3.2 Structural and Function Relationship

Studying dendritic trees reveals mechanisms of function in a neuron in terms of its connectivity and computation. Neurons of different types serving different functions should noticeably differ in the morphology and/or physiology of their dendrites. Indeed, up to this day, dendrite morphology represents one of the main criteria for classification of neurons into individual types [15]. At the same time, due to its wide implication in neuronal functioning, dendritic morphology plays a role in many pathological cases, as stated in section 1.1. Different facets of neural function can therefore be studied directly taking advantage of knowledge of dendrite morphology: the role of different cell types, malfunctions in nervous tissue, development of neural function, and emergence of function

in the single cell and in the circuitry. For all these reasons, neuronal morphology lies at the core of many studies in neuroscience.

3.2.1 Neuronal Morphometry

Quantitative measures of neurite morphology are extracted from microscopy data. After an initial stage in which neuronal tissue is prepared and neurons are stained or labelled, a neuron most prominent features are accessible by visually inspecting it under the microscope. Some general features such as overall size, spatial embedding, and branching complexity can already be resolved at this stage, but for a thorough quantification of the dendrite structure, a reconstruction, i.e., a digital representation of the morphology is required.

This step is named *tracing*, and there are many softwares packages which accomplish this reconstruction in a automatic way, the most used is Neurolucida (proprietary), [47] but there are many freely available tools such as the TREES Toolbox [25], amongst others [47]. In principle, these reconstructions of morphologies from neural tissue preparations could provide objective criteria and relieve the human labor associated with manual reconstruction. However, none of the software packages available at present provide tools to flawlessly reconstruct the entire cell, and manual intervention is still required in most cases because of histological, optical and operator-linked distortions.

All these experimental data are continuously being accumulated and put into a digital format, but there are very few archives that are publicly available through the Internet to make this data readily accessible. Several labs host their own databases that can be accessed through the Internet, but the most complete database is NeuroMorpho.org [78]. In this database thousands of morphology files from a large number of different labs, are available freely in the public domain in a standardized `.swc` format.

In the `.swc` format [18], neuronal morphology is a set of connected nodes directed away from a *root* node. Since each node is attributed one diameter value, the segments in the graph each describes a truncated cone (*frustum*), where the starting diameter of one frustum is the ending diameter of the parent frustum. The morphologies are encoded as plain ASCII text files that contain seven values to describe each node: (1) the node index starting at the value; (2) a region code describing whether a node belongs to the soma, the dendrite, or any other region of the neuron; (3–5) x, y, z coordinates; (6) the diameter at the node location; and (7) the index of the parent node. In principle, most neuronal structures can be represented in sufficient detail with this approach.

Once the digital reconstructions are obtained and stored, they can be used for further analysis and quantification and be used to address distinct research questions. **Morphometry**, the quantitative study of neuronal structures, can be divided into two main categories: **topological** and **geometric** morphometrics.

Topological Measures

Topological analyses disregard the metric features and describe the connections in the dendritic tree structure. Quantitative description of branching structures is well developed in graph theory. A graph Γ is a pair (V, E) o a finite set V of vertices or nodes and a set E of unordered pairs, called edges or links, of different elements of V. Thus, when there is an edge $e = (i, j)$ for $i, j \in V$, we say that i and j are connected by the edge e and that they are neighbours, $i\ j$. A special type of graph in which the edges do not form loops is called a tree, i.e., $\forall e \in E, e \neq (i, i)$.

This abstract object is put in correspondence to a neuronal tree, where the three types of vertexes are the *root*, the *branch point* and the *terminal tips*. The two types of elements connecting the vertexes are *intermediate segments* and *terminal segments*. The *root* is the point of origin of the tree, located conventionally at the soma. The *branch point* is the vertex into which one segment enters and two or more segments exit. It is said that, at the branch point, the parent segment gives rise to two or more daughter segments. Such a branch point is called a *bifurcation* or *multifurcation* point. If all branch points of a tree are bifurcations then the tree is *binary* (which is the case for real dendrites). A part of the tree composed of a certain subset of connected branches and vertexes is called the *subtree*.

Particularly, one of the most used measures for quantitatively distinguish dendrites has been *partition asymmetry* that assesses the topological complexity of a neuronal tree based on the normalized difference between the degree of two daughter subtrees at a branch point. The partition asymmetry index ranges from 0 (completely symmetric) to 1 (completely asymmetric) [91]. The partition asymmetry index A_p is defined as:

$$A_p = \frac{|r - s|}{r + s - 2} \tag{3.1}$$

with r and s indicating the number of terminal tips of each subtree, where $r \geq s$, and indicates the relative difference in the number of branch points $(r - 1)$ and $(s - 1)$ between the subtrees. This indicator does not allow one to distinguish all the tree types of the same degree, however, other measures have even less discriminative power [64].

Measure	Definition
Number of stems	Total number of segments leaving from the dendritic root
Number of branch points	Total number of branch points in thre tree
Branch order	Topological distance from the dendritic root
Degree	Termination points downstream of the node under investigation
Partition asymmetry	Topological complexity of a tree

Table 3.1: List of frequently used morphometric measures to quantify neuronal topology [24].

Metrical Measures

In contrast to topological properties that have no metric interpretation, geometric properties consider the spatial embedding of a tree. Metrical parameters which characterize the

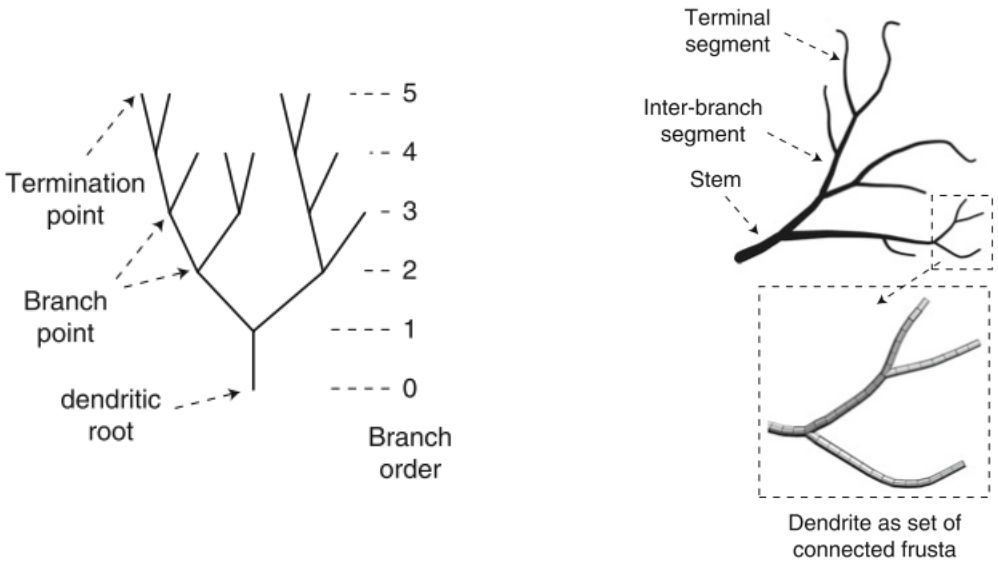

Figure 3.2: **Left image** - Topological analyses disregard the metric features and describe the connections in the graph underlying the dendritic tree structure. **Right image** - For a geometrical analysis, the tree is embedded in space and length values play a role (this picture was from [24]).

extent and thickness of the dendritic segments are the segment length, the diameter and the membrane area. The lengths of individual segments allow the construction of the cell metrical variables used in morphometrical studies and in simulations of electrical and electrodiffusive properties of neurons. Such variables are the total *dendritic length*, which is the sum of lengths of all segments constituting the dendritic arborization and the *path length*, which is the sum of lengths of the consecutive segments forming the path between a given origin and a terminal point, e.g., between the root and a certain terminal tip. Nevertheless, this review of metrical measures is far from exhaustive, since morphological and morphometrical studies of neural shape and texture are becoming more and more important in the field of neurosciences due to the recognized close link between shape and function at molecular, cellular and tissutal level, more exotic measures started to appear on the literature [81].

Measure	**Definition**
Total length	Summed segment lengths of all segments in a tree
Segment length	Path length of the incoming segment toward a node
Dimension	Width, height, and depth of the bounding box
Taper rate	The uniform decrease in diameter across a dendritic branch

Table 3.2: List of frequently used morphometric measures to quantify neuronal metrics [24].

3.2.2 Structure Influences Function Hypothesis

In addition to ion-channel composition, dendritic morphology appears to be an important factor modulating firing pattern. In many cell types, including neocortical and hippocampal

pyramidal cells, neuronal firing patterns are correlated with dendritic morphology. Results from modelling studies also suggest a relationship between dendritic morphology and firing pattern (e.g. [70, 88]). It has long been assumed that neuroanatomical variability has an effect on the neuronal response, but not until the last decade it was attempted to quantify these effects. Furthermore, in electrophysiological studies, usually the neuroanatomy is rarely quantified, and in neuroanatomical studies electrophysiological response is rarely properly measured.

Particularly, computational techniques have the potential of bridging the gap between electrophysiology and anatomy, and testing the morphology influences physiology hypothesis. Computational techniques include modelling of neurophysiology, modelling and measurement of neuroanatomy, and mining publicly available archives of anatomical and electrophysiological data. Indeed, the neuromorphology effects on neurophysiology usually is studied by mining electronic archives for neuroanatomical data, utilizing computational modelling techniques to simulate neuronal firing behavior, and quantifying the effect by correlating the morphometrics described above with electrophysiological measurements of simulations. The general method consists of converting morphological measurements from 3D neuroanatomical data into a computational simulator format. In the simulation, active channels are distributed evenly across the cells so that the electrophysiological differences observed in the neurons would only be due to morphological differences. The cell morphometrics and the cell electrophysiology in response to current injections are measured and analysed.

However, the majority of these studies are mainly correlative [2, 11, 70, 87, 92] , focus on morphologically very distinct cell classes, use only the physiologically less appropriate stimulation protocol of somatic current injection, and make no distinction between the two sources of morphological variability: metrics and topology, and consequently, the effects of dendritic size and topology on firing patterns, and the underlying mechanisms, remain poorly known.

Remarkable exceptions, on the topological side, are [30, 88, 89], in these studies the influence of dendritic topology on the generation of specific firing patterns was systematically addressed. Basically, what one can infer from this studies is that topological differences (measured from *partition asymmetry index*) may function as an on-off switch for certain firing patterns such as *bursting*.

On the other hand, exceptions on the metrical side are [61, 62, 64, 63, 65]. In these, metrical differences are quantified, and then how these differences influence the propagation of electrical current from the dendrites to the soma is analysed. This allowed the introduction of some biophysically based criterion for the electrical distinction between metrically (a)symmetrical dendritic branches.

Problem: Linking Geometry, Topology and Function

When trees are equivalent in their topology but clearly distinct in metrical sizes (e.g. in length or thickness), undoubtedly the topological quantitative characterization of trees is not sufficient to classify the dendritic structure, and vice-versa. For example, unequally long segments may form unequally or equally long multisegment paths; the metrical description is further complicated by differences in diameters which exist even between equally long segments, and all these differences have influence on the electrical behaviour of the cell.

Moreover, although metrical differences between subtrees happen as often as differences in topology, quantitative indicators of metrical symmetry/asymmetry are far less elaborate than those used in topology studies. The need for some complementary description of metrical properties has not yet been met, and neither quantitative measures that combine both kinds of measures [64].

3.2.3 Electrotonic Distance

What one can realise from these previous mentioned studies, is that unfortunately, it is difficult to infer and analyse how neuronal form affects electrical signaling because of the different parameters that have to be taken into account. As new metrics and more cells are put in the analysis, the parameter space has the potential of exploding and making analysis undoable, specially if one wants to account for topological and metrical factors.

For this reason, it was developed a quantitative yet intuitive approach to the analysis of electrotonus of neuron that takes into account certain morphological aspects. This approach transforms the architecture of the cell from anatomical to electrotonic space, making a connection between morphology and function [58, 79].

Classic Electrotonic Distance

The *electrotonic distance* can characterize the efficiency, or the degree of coupling, between any particular synaptic input site and the cell body where the initiation of the action potential occurs. This measure is defined as the physical distance x scaled by the length constant λ[1] :

$$X = \frac{x}{\lambda}. \tag{3.2}$$

Similarly, the electrotonic length of a finite cable (i.e. dendrite) is the total length l scaled by the length constant

$$L = \frac{l}{\lambda}. \tag{3.3}$$

[1]The voltage decreases to e^{-1}, that is, to 37% of its original value, at λ and to e^{-2}, or 13% of its original value at 2λ, and so on

A more general expression for X between two points i and j, applicable to cables of varying geometry or membrane properties, is

$$X = \int_{x_i}^{x_j} \frac{dx}{\lambda(x)}. \tag{3.4}$$

However,this measure is misleading. In an infinite cylinder, there exists a simple exponential relationship between the electrotonic length and the voltage attenuation. In all other structures, it does not provide a measure of the efficacy of signal transfer, since the underlying space constant assumes the convenient fiction of an infinite and constant cylinder. So, depending on the type of boundary condition imposed, the actual voltage attenuation in a cable can be stronger (for a *killed-end*) or weaker (for a *sealed-end*) than in an infinite cylinder with the same diameter and membrane parameters. This difference can be substantial in real trees, given the heavy load imposed by all the additional branching [60].

New Electrotonic Distance

The new electrotonic distance always has a simple, direct relationship to attenuation, regardless of cellular anatomy, whereas the classical measure only has meaning in cells that meet several very specific constraints [19, 95]. Let i and j be spatial indices along a branched structure without loops. The *voltage attenuation* between two points i and j is defined as,

$$A_{ij} = \frac{V_i}{V_j} \tag{3.5}$$

where the first subscript i gives voltage at the location of the current input, and the second subscript j the voltage at the location of the recording electrode. Then, taking the logarithm *log-attenuation* is defined as,

$$L_{ij} = \ln A_{ij} = \ln \frac{V_i}{V_j} \tag{3.6}$$

A general expression L_{ij} analogous to equation (3.3) is

$$L_{ij} = \int_{x_i}^{x_j} \frac{dx}{\lambda_{eff}(x)} \tag{3.7}$$

where the *effective space constant* $\lambda_{eff} = |V(f = 0, x)/(dV(f = 0, x)/dx)|$ is the functional generalization of the classical definition for λ

Properties

Here we catalogue briefly some important properties of the quantities defined above that will be useful in interpreting the morphoelectrotonic transform:

1. The *log-attenuation* is not in general symmetric:

$$L_{ij} \neq L_{ji} \tag{3.8}$$

2. Since the response is always greatest at the site of injection, $V_i \geq V_j$ so that $L_{ij} \geq 0$.

3. If a point j is on-path from i to k, then the total *log-attenuation* is just the sum of the respective partial measures. That is, the *log-attenuation* is additive for j between i and k,

$$L_{ik} = L_{ij} + L_{jk}. \tag{3.9}$$

This property allows the introduction of a sort of pseudo attenuation metric. Additivity constitutes a feature of *log-attenuation*, rendering it somewhat similar to a distance measure[2]. Because the *log-attenuation* between two points in an infinite cable equals the electrotonic distance between them, L_{ij} can be viewed as a generalization of the traditional notion of electrotonic distance to arbitrary cable structures.

Can this measure, be used to develop a quantitative approach to measure dendritc structure that does not directly takes into account the physical parameters of the architecture of the cell, but considers instead this electroctonic space as a pseudo metric, and by doing solve the problem stated previously? This hypothesis will be further explored in the next chapter.

3.3 Summary

In this chapter, we reviewed the field of structure-function relation in Neuroscience, particularly the topic of dendritic shape. First, we start by introducing two not opposing views of dendritic shape paradigms, and then we move to explain how this structures can be quantitatively measured. Afterwards, there was exposed the state of the art on how these measures are being used to elucidate the link between structure and function in single neurons. In the end of the chapter, some tensions and future prospects in the field were analysed.

[2]Note that L_{ij} is not a true metric, since symmetry does not hold due to the asymmetry in the voltage attenuation.

Chapter 4

A New Structural Measure

In this chapter we derive and introduce a new measure that relates structure to function. We develop a quantitative approach that does not directly takes into account the physical properties of the architecture of the cell (i.e. anatomical variables and ion channel composition), but instead considers the electrotonic distance of the cell as the metric, and by doing so we are able to reduce some of the parameters to be analysed, while creating a bridge between structure and function.

To the best of our knowledge, the contribution presented here is novel in three aspects: *(i)* this measure can account for variations in metrical, topological and biophysical components of the cell whole at the same time; *(ii)* it uses a rather abstract framework for quantifying structural differences and because of the previous *(iii)* it has a highly discrimanitive power.

In section 4.3., using the new measure we are at position of fully address the the question of how synaptic efficacy is affected by the anatomical and biophysical properties of the postsynaptic cell, and we hypothesise a new mechanism for current synchronization in dendrites, making predictions that are experimentally testable.

4.1 Symmetry

The concept of *symmetry* is a fundamental one in science. Symmetry is important not only as a tool in structure determination in physics, chemistry, biology [29, 31, 76], but as a basis for understanding dynamical processes as well [71].

Everyone has some idea of what symmetry is, for instance, we recognize the bilateral (left-right) symmetry of the human body, of the bodies of many other animals, and of numerous objects in our environment. The word symmetry commonly refers to the fact that the shapes and dimensions of some objects repeat themselves in different parts of the object, or when the object is viewed from different perspectives.

In science, of course, the recognition and utilization of symmetry is often more sophisticated, but what symmetry actually boils down to in the final analysis is that, if the situation/structure possesses the possibility of a change that leaves some aspect of the

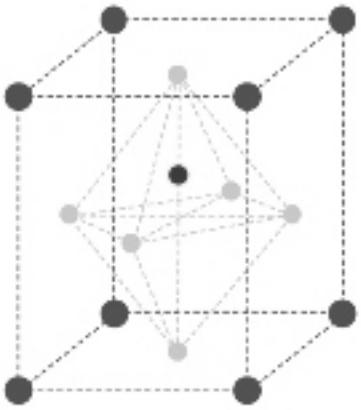

Figure 4.1: Diagram of the Perovskite crystal structure. Due to the spatial symmetry of crystals, many important physical properties of a crystalline material depend on the orientation of the sample with respect to some specifically defined coordinate directions. Examples of such properties are electrical conductivity, elasticity, the piezoelectric effect, and nonlinear optics [31].

situation/structure unchanged we have symmetry, i.e., symmetry is immunity to a possible change. On the other hand, if a change is possible but some aspect of the situation is not immune to it, we have asymmetry.

If a change is made to a physical system, either a discrete object or a mathematical formula describing a physical property, this is called a *transformation*. If a system appears to be exactly the same before and after the transformation, it is said to be *invariant* under that transformation. Symmetry in nature plays a critical role in everything from our understanding of the nature of elementary particles to our models of the structure of galaxies in the universe. Almost all of the laws of nature have their root in some type of symmetry. Because of this, if we elucidate the symmetry of a physical system we can predict many of its physical properties [71].

In modern times, symmetry is defined mathematically by *Group Theory*. In Group Theory symmetry becomes a universal property of mathematical structures, for instance, the symmetry of a set (e.g. points, numbers, functions) is defined by the group of self-mappings (automorphisms) that leaves unchanged the structure of the set (e.g. proportional relations in Euclidean space, arithmetical rules of numbers, etc.). The application of Group Theory allows the determination of many of the physical properties of that system and some of these properties correlate with functional properties of the system (e.g. see Figure 4.1) [23, 28, 40]. Therefore, symmetry seems an appropriate concept to help fully quantify the structural differences between dendritic trees that latter may play a role in neuronal function. Basically, the more symmetric a dendritic tree is, the more similar its branches and branching pattern should be, and the other way around for asymmetrical trees. But how can one apply such concept to dendritic trees?

4.2 Dendritic Tree as a Graph

A graph is the mathematical structure representing binary relationships between discrete elements (see subsection 3.2.1). These elements are the *vertices* of the graph, and the relationships are encoded as connections or *edges* between vertices. Such a graph can then be a network, that is, the substrate of dynamical interactions carried by the edges between processes located at the vertices [55].

Particularly, as a graph, a tree is represented by a set of labelled nodes connected by edges. Since most statistics describing a neurons branching relate to the root (e.g. branch order, which increases after each branch point on the way from the tree root to all terminal nodes) it makes sense to attribute a directionality to the edges and to define the root as the node with the *index* 1. All edges lead away from the root, that defines their directionality uniquely.

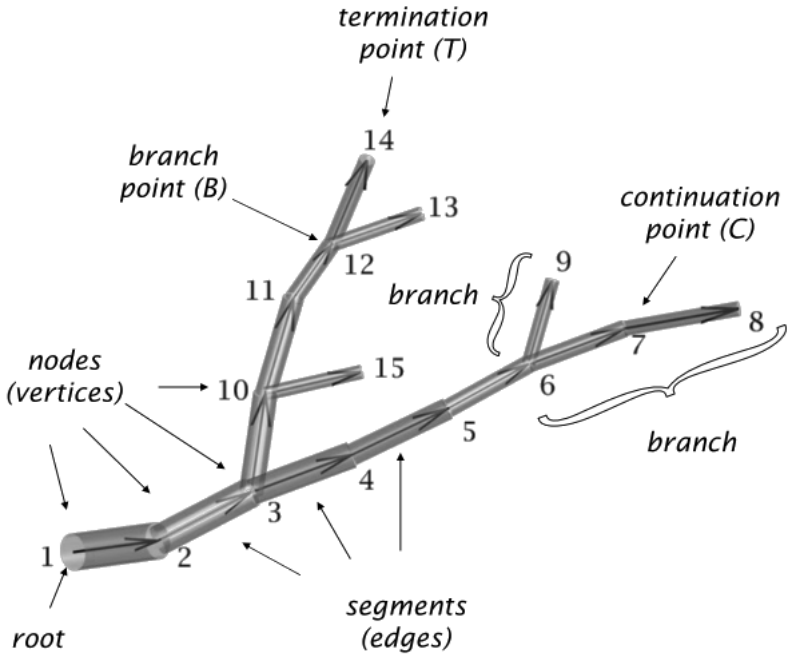

Figure 4.2: Example of how a dendritic tree is represented by a set of labelled nodes connected by edges in a graph. There are four different types of nodes: *root* of the graph is the meeting point for the dendrites and the soma, *leafs* (or *tips*) of the graph are defined as the termination points of the dendrites, the *binary branching nodes* of the graph are defined as the dendrites branching points, and the continuation points, are nodes used to account for *frustum* in certain software packages. A dendritic branch begins at the root (i.e. the stem branch) or with a branching point, and it ends with another branching point or a terminal point [25].

When neuronal trees are regarded as graphs, their branching structure can be well described with the corresponding directed adjacency matrix dA, a quadratic matrix of size NxN, where N is the number of nodes in the tree. As mentioned earlier, the direction of the edges shows away from the first point, representing the arbitrary starting vertex $S = 1$, the root of the tree. Note that the widely used `.swc` format for storing neuronal morphology is nothing else than a sparse representation of the adjacency matrix since it

simply attributes to all nodes (row index) a parent node (column index). Of course, most large graphs arising in applications are sparse, that is, between most pairs i, j, there is no edge. This means that most of the entries of the adjacency matrix are $0's$. For example, the following tree with $N = 8$,

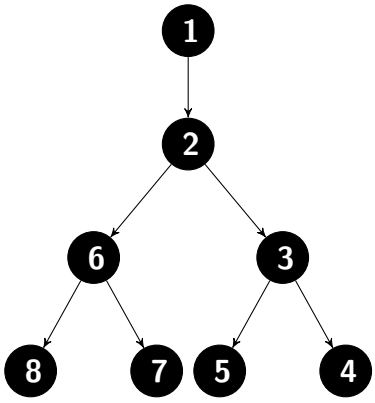

will have the following adjacency matrix:

$$\begin{pmatrix} 0 & 0 & 0 & 0 & 0 & 0 & 0 & 0 \\ 1 & 0 & 0 & 0 & 0 & 0 & 0 & 0 \\ 0 & 1 & 0 & 0 & 0 & 0 & 0 & 0 \\ 0 & 0 & 1 & 0 & 0 & 0 & 0 & 0 \\ 0 & 0 & 1 & 0 & 0 & 0 & 0 & 0 \\ 0 & 1 & 0 & 0 & 0 & 0 & 0 & 0 \\ 0 & 0 & 0 & 0 & 0 & 1 & 0 & 0 \\ 0 & 0 & 0 & 0 & 0 & 1 & 0 & 0 \end{pmatrix}$$

Not each possible directed adjacency matrix represents a possible neuronal tree, since loops and branching points with more than two child branches are possible, but do not exist in natural dendritic trees. Therefore, dA never contains more than two entries in one column and no entry will lay directly on the diagonal. Also, each node has exactly one parent, apart from the root, which has none. Each row of dA therefore contains exactly one entry apart from the first, which contains none. If for some reason, it is necessary to better describe the relation between nodes *weights* can be attributed to edges, and instead of $1's$ in dA we simply put a specific number instead. In order to derive most dendritic branching statistics using the typical descriptions, an algorithmic formulation by recursion is required to walk through dA and collect statistics, and by doing so, formal measures can be applied to dendritic structures.

4.2.1 Algebraic Graph Theory

After translate a dendritic tree into a graph, it becomes possible to to apply the concept of symmetry to trees through **Algebraic Graph Theory** [10, 13, 39, 42].

There are two main connections between graph theory and algebra. These arise from two algebraic objects associated with a graph, its adjacency matrix and its *automorphism group*:

1. In one, the automorphism group of a graph can be regarded as the collection of all permutation matrices that commute with the adjacency matrix, and provides a way to study symmetry in graphs.

2. The other one, **Spectral Graph Theory**, is the study of properties of a graph in relationship to the *characteristic polynomial*, *eigenvalues*, and *eigenvectors* of matrices associated to the graph, such as its adjacency matrix. This topic will not be covered in the present manuscript.

An *isomorphism* between graphs $\Gamma_1 = (V_1, E_1), \Gamma_2 = (V_2, E_2)$ is a bijection $\Phi : V_1 \to V_2$ that preserves neighbourhood relations, that is, $i \sim j$ iff $\Phi(i) \sim \Phi(j)$. In other words, i and j are connected by an edge precisely if their images under Φ are. Isomorphisms preserve the degrees of vertices, that is, $n_i = n_{\Phi(i)}$ for every vertex i. An *automorphism* of Γ is an isomorphism from Γ onto itself. The identity map of the vertex set of Γ is obviously an automorphism, but there may or may not be others, depending on the structure of Γ. The automorphisms of Γ form a group under *composition*. We can then quantify the symmetry of Γ as the order of its automorphism group, i.e., a bigger the order means more symmetry.

From these definitions, another key concept in Algebraic Graph Theory arises:

- **Edge Automorphism**- An edge automorphism of a graph Γ is a permutation of the edges of Γ that sends edges with common endpoint into edges with a common endpoint. The set of all edge automorphisms of Γ from a group called the *edge automophism group* of Γ. Furthermore, if the edges have weights, then for the permutation to happens the edges must have equal weights.

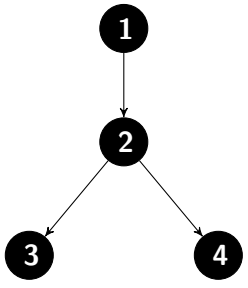

Figure 4.3: The star graph S_4 has six vertex automorphisms: $(3, 4, 1, 2)$, $(3, 1, 4, 2)$, $(4, 3, 1, 2)$, $(4, 1, 3, 2)$, $(1, 3, 4, 2)$, $(1, 4, 3, 2)$.

4.3 The new Measure

As previously mentioned, the topology of a tree is determined by the connectivity pattern of its segments, and its metric properties are the geometrical values of its branches. If one translated a dendritic tree to a graph, branching points would be vertices of that graph, and branches would be edges (i.e. the graph would be embbeded in metric, and weights w_{ij} would be atributed to edges). In this terms, a dendritic tree could be formalised as a graph, and its properties encoded in its adjacency matrix, opening the opportunity of exploring it with formal graph theoretical measures.

Obviously, similarities or differences in electrical states of dendritic parts are accompanied by smaller or greater heterogeneity of topological and metrical parameters of the arborizations, making these structural variations central to the understanding of the observed phenomena. Therefore, the study of its symetrical properties would enable one to fully quantify this heterogeneity, where the more symmetric a dendritic tree is, the more similar its branches and branching pattern should be, and the other way around for asymmetrical trees. This could be quantified by vertex automorphism, for topological patterns, and by edge automorphism, for metrical parameters.

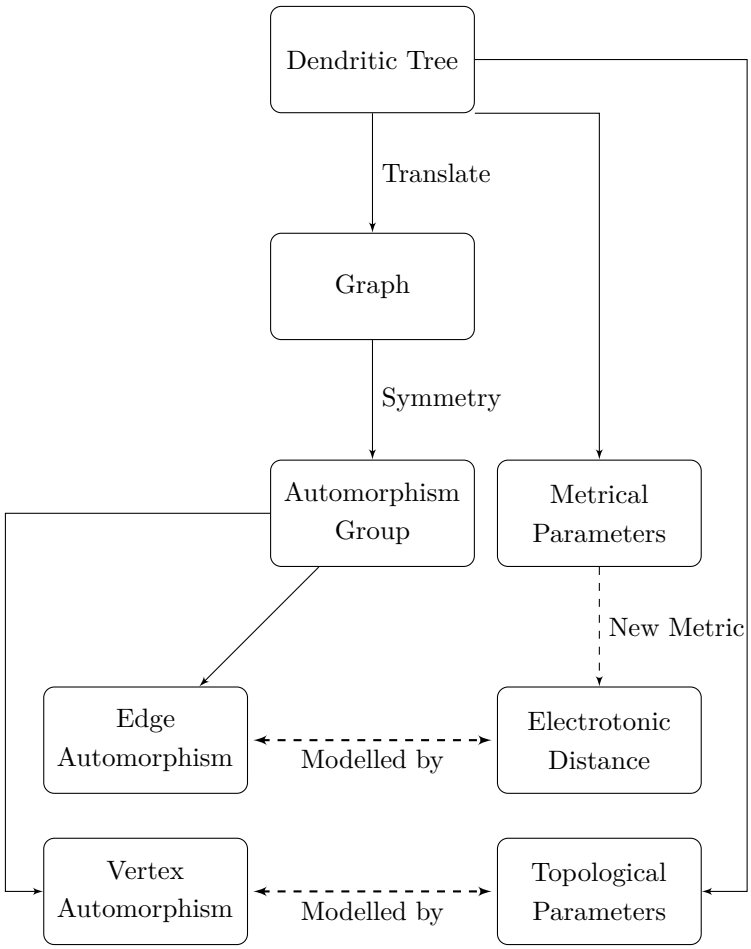

Nevertheless, the attribution of a single number w_{ij} that establishes the relationship between nodes is non-trivial for two reasons:

- Metrical parameter transition to the adjacency matrix is not trivial because a branch may vary in many different variables, such as, length or diameter.

- Ion channel composition of a dendritic tree affect the electrical behaviour of the cell, but these are orthogonal to structural parameters, what can blur the structural-function relationship [4, 5, 48, 54, 75]

To solve this problem, the graph that represents the dendritic tree may be *embedded* in a new metric, that not only takes into account the physical variables of the cell (i.e. anatomical variables), but instead considers the electrotonic distance as the distance metric, and by doing so reduce some of the parameters to be analyzed, and providing a direct relation between structure and function, i.e., each weight of dA would be $w_{ij} = L_{ij}$, the electrotonic distance of that branch. This approach clearly provides a link between structure and function.

Measure e^{-X}

At first sight, the concept of a tree as defined above seems appropriate for that task. However, when one wants to operationalize this idea Group Theory is too *stiff* for this task because, *(i)* a graph when embedded in a metric, the exact spatial symmetry limit of the edges needed to perform the permutations, it is obviously unobtainable in practice due to the influence of small, random fluctuations in physical systems, making edge automorphism a virtual impossible condition to be satisfied. Moreover if the measure wants to be discriminative it needs to account for bigger or smaller levels of more or less symmetry. On top of that, *(ii)* algebraic graph theory in general, and computational algebraic graph theory in particular are more concerned in the generation of graphs, than on the analysis of graphs, making the analysis of the dendritic trees a practical problem as well for implementation reasons [14, 36, 74].

What one needs to overcome this hurdle, is a measure that could mimics vertex and edge automorphism concepts, while being sensitive to different levels of (a)symmetry, and being easily computed and implemented, therefore:

1. If one considers the simplest dendritic tree, with a single branching point, this tree is translated into a graph with four nodes, the soma (s) the root of the branching point r and two daughters d_1 and d_2 nodes, each one connected to the root by an edge, namely w_{rd_1} and w_{rd_2}. Following from algebraic graph theory, a permutation between d_1 and d_2 would be possible *iff* the neighbourhood relations between all nodes would stay the same (condition trivially satisfied in this particular case) and edge automorphism must be verified as well, and for the later $w_{rd_1} = w_{rd_2}$ must hold. Taking this example to a more practical case, a dendritic tree constituted by a simple branching point, if the two daughter branches have the same electrotonic distance this corresponds to the most symmetrical case for the total wiring length of

$w_{rd_1} + w_{rd_2}$. For the total wiring length of $w_{rd_1} + w_{rd_2}$, the bigger the height (i.e. the distance from the root to one of the nodes) of either d_1 or d_2, the more asymmetric the tree will be. This notions of (a)symmetry can therefore be expressed in the form of a simple ratio between the distances between both edges of the branching point. In the symmetrical one will have $ratio = d_1/d_2 = 1$, and in the asymmetrical cases one will have $ratio < 1$ ($ratio \to 1$ as it gets increasingly more symmetrical and $ratio \to 0$ as it gets increasingly more asymmetrical).

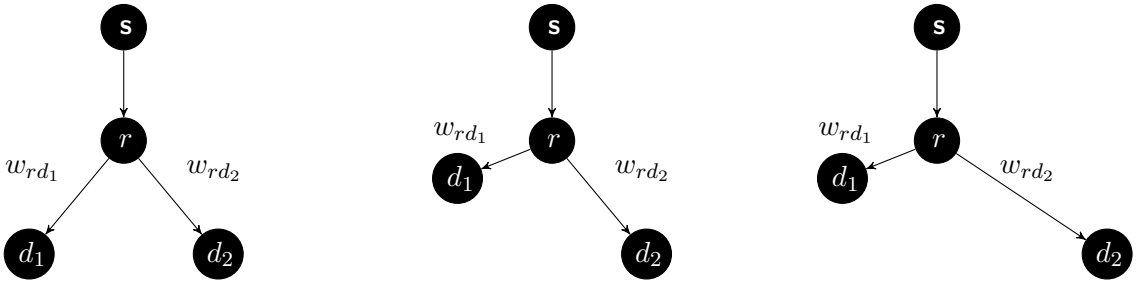

Figure 4.4: Symmetry ratio visualization

2. However, the electronic coupling between dendritic branches not only depends on the degree of (a)symmetry between them, but size plays a role too. Even for branching patterns that hold the same ratio, differences in total electrotonic distance influences the coupling of these structures, with bigger total wiring lengths promoting more signal attenuation, and vice-versa (see section 3.2.3). To overcome this situation, the ratio defined above can be altered to $\dfrac{w_{rd_1}/w_{rd_2}}{w_{rd_1} + w_{rd_2}}$ this way when the total wiring length is the same, the difference between the asymmetrical and symmetrical patterns will be the same as in the previous ratio, but at the sime time differences in the total electrotonic structures are take into account as well. In this new formulation as $w_{rd_1} + w_{rd_2} \to 0$ the bigger the electrotonic coupling will be, and as $w_{rd_1} + w_{rd_2} \to \infty$ the smaller the electrotonic coupling will be.

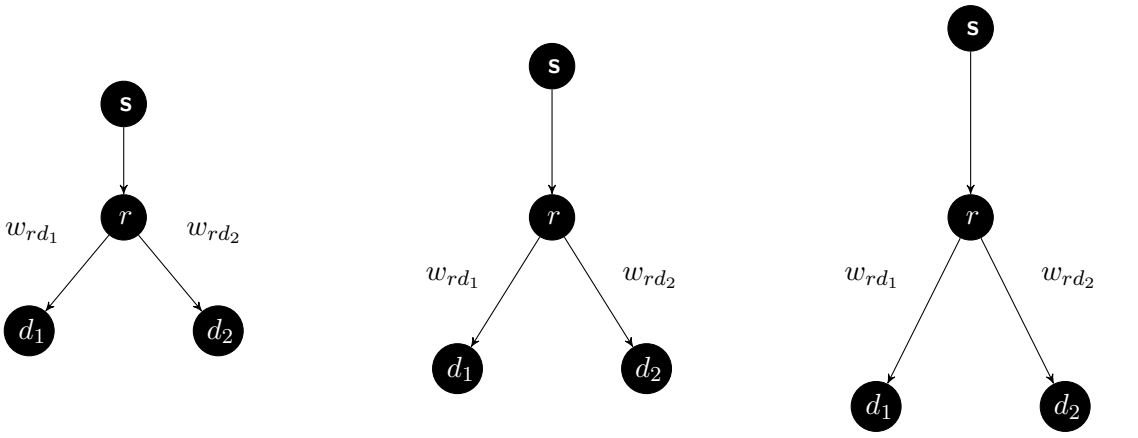

Figure 4.5: Size effect visualization. The trees represented in this figure are scaled up versions of the first tree. If the symmetry ratio defined above was not normalised these trees would have virtually the same electrotonic structure.

3. From graph theory one knows that a binary tree can be decomposed or generated from a set of subtrees, and since the electrotonic distance enjoys the property of additivity (see equation 3.9) the structure of an arbitrarily complex dendritic tree can be computed using the information from each of its subtrees in a recursive way.

4. Following 1, 2 and 3 to quantify the electrotonic extent of a dendritic tree, we introduce a new measure called e^{-X}. For a given binary dendritic tree with N nodes, we compute and sum for each internal node i_n, the ratio defined below:

$$X = \begin{cases} \sum_{i=1}^{i_n} \dfrac{w_{r_i}/w_{l_i}}{w_{t_i}} & \text{, if } w_{r_i} \geq w_{l_i} \\ \\ \sum_{i=1}^{i_n} \dfrac{w_{l_i}/w_{r_i}}{w_{t_i}} & \text{, if } w_{l_i} > w_{r_i} \end{cases} \tag{4.1}$$

where w_{r_i} is the sum of all electrotonic paths P_{r_i} of the right subtree rooted at the given internal node, computed from the soma to each leaf of this subtree,

$$w_{r_i} = \sum_{r_{i=1}}^{n_{r_i}} P_{r_i} \tag{4.2}$$

the same holds for w_{l_i},

$$w_{l_i} = \sum_{l_{i=1}}^{n_{l_i}} P_{l_i} \tag{4.3}$$

and,

$$w_{t_i} = w_{r_i} + w_{l_i} \tag{4.4}$$

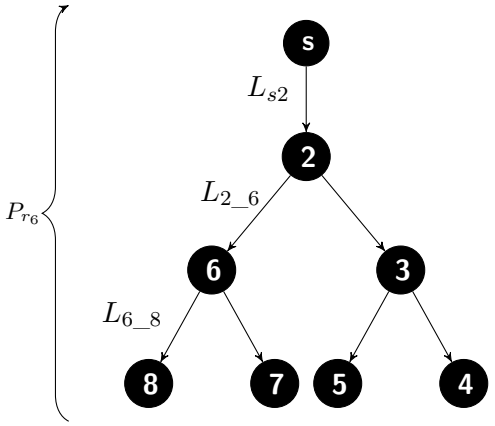

Figure 4.6: Illustration of the only electrototonic path of the right subtree rooted at node 6 (P_{r_6}) of the left tree. The tree has three internal nodes: 2, 3, 6.

5. So, when $P_{r_i} \to 0$, i.e. when electrotonic distance is decreasing and electrotonic coupling is increasing, $X \to \infty$ and $e^{-X} \to 0$, and when $P_{r_i} \to \infty$, i.e. when electrotonic distance is increasing and electrotonic coupling is decreasing, $X \to 0$ and $e^{-X} \to 1$, therefore one may interpret e^{-X}, as a generalised measure of signal attenuation that takes into account the structure of the neuron. When $e^{-X} = 0$ there

is no signal attenuation, and when $e^{-X} = 1$ the signal attenuation is maximal and there is no signal reaching the soma[1] .

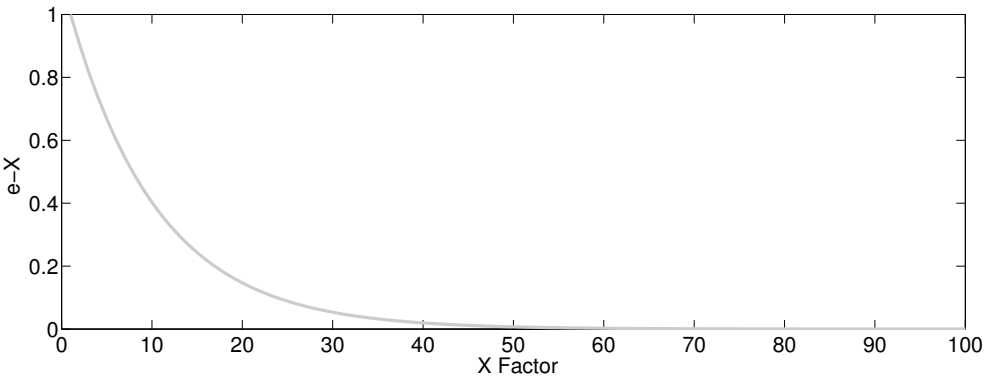

Figure 4.7: e^{-X} and X factor relation. X is the structural factor that depends on the tree's metrical and topological information, and it is exponentiated for data visualization purposes and to facilitate data analysis.

4.3.1 Hypothesis

From what was stated in the previous subsection, one can easily postulate another corollary that straightforwardly emerges from the analysis of e^{-X}: if the size effect P_{r_i} is the same across different cells, and the symmetry factor is the only varying factor, when $ratio \to 1$, i.e., the more symmetric condition, X will be bigger than when $ratio \to 0$, i.e., more asymmetric condition, therefore $e^{-X_{sym}} < e^{-X_{asym}}$. Therefore, since e^{-X} is a generalised measure of signal attenuation, one can conclude that in more symmetrical structures the attenuation is smaller than in more asymmetrical conditions.

Nature is assumed to be causal, and when organisational patterns are observed in Nature usually they are the basis of similar functions, behaviour or dynamics. Given a particular set of physical circumstances the same physical behaviour is expected to occur whenever and wherever these structures are repeated. So symmetry in terms of a neuron's electrotonic structure, seems to play an important role in signal integration, being a possible mechanism for the modulation of axial current that flows from the dendrites to the soma. The biophysical substrate for this hypothesis is **synchronization**, because the electrotonic structure of the cell is more symmetric, it implies that the electrical behaviour of the cell will be similar, i.e., the current flowing from different paths will have similar dynamics, and because of that will spatially sum in a more efficient way. Therefore, we are at position to state the following testable **experimental predictions**:

1. more symmetric electrotonic structures will achieve higher levels of current measured at the soma, other things being equal.

[1] e^{-X} is a measure of synaptic efficiency, it should not be forgotten that it represents a relative measure, and whether or not the cell spikes by exceeding a threshold depends on the absolute amplitude of the somatic PSPs

2. these different levels of current measured at the soma will be translated into different output behaviours of the cell.

   and the following **methodological prediction**:

3. Measure e^{-X} will be discriminative across different neuron types, when other frequently used measures are not (see appendix A).

4.4 Summary

In this chapter, we introduced a new structural measure for synaptic efficiency. First, we started by reviewing the field of Algebraic Graph Theory, and introduced some key concepts of the area that are behind the *rationale* of the new measure. Afterwards, we derived the new measure e^{-X} that solves the problem stated in the previous chapter. In the end of the chapter, and supported on this new measure two experimental predictions, and a methodological one were made.

Chapter 5

Simulations

In this chapter we give a description of the approach and method used to test the predictions and hypothesis stated in section 4.3.1, concerning the validity of the measure e^{-X}. This chapter consists of four main sections. In section 5.1., an overview of the experimental conditions is provided. In Section 5.2, we expose the artificial reconstruction process of the simulated neurons that we use to manipulate the synchronization mechanism. In section 5.3, we describe the simulation-based experiments performed to test the stated predictions and hypothesis. Finally, in section 5.4, we show the core results of the thesis and the statistical analysis of the data. The results show that the proposed synchronization mechanism is a robust and important factor modulating axial current that causes neurons to spike.

5.1 Experimental Conditions Overview

Since realistic modelling of single neurons has reached a relatively mature phase, we took advantage of the capability of such models to simulate conditions that are difficult to test experimentally. Three different types of neurons were collected by examining electronic archives of neuroanatomical data, and for each neuron type, the dendritic trees were artificially modified, while maintaining the same total wiring lengths, with the intention of causing changes at the electrotonic structure of the cell in terms of (a)symmetry. Moreover, each neuron type differs in its total wiring length, so one can investigate how size, and different topologies influences the processing of synaptic inputs in a dendritic tree, while at the same time verify the discriminative power of measure e^{-X}. In the simulations, active channels are distributed across the cells to achieve greater biophysical realism, and then electrophysiological differences observed in the neurons are measured and compared with e^{-X} values. The analysis and model code for this thesis is available in the accompanying cd-ROM.

To test the hypothesis stated in the last chapter in a systematic way, two different conditions were simulated: **Axial current condition**- the amount of axial current reaching the soma from the dendrites is measured. **Spike train condition**- voltage traces

are measured at the axo-somatic compartment to collect spiking patterns.

5.2 Artificial Reconstructions

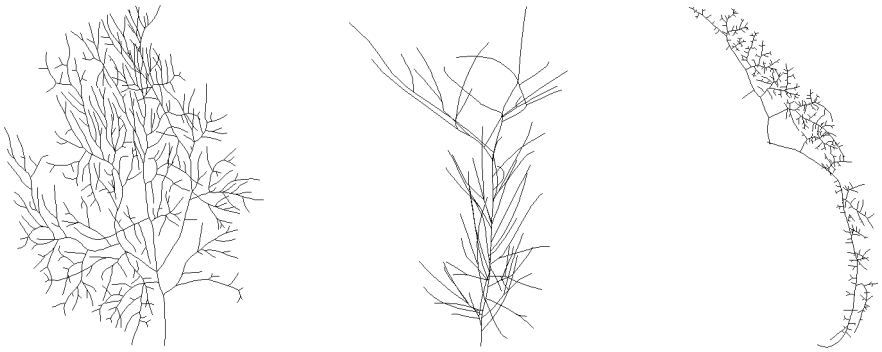

Figure 5.1: Shape diagram of the original collected neurons.

	Purkinje	**Pyramidal**	**Visual**
Total wiring length (μm)	5759.001	8483.71	4278.82
Branching Points	299	60	327
Terminal Tips	300	61	328
Number of stems	1	1	1
Number of branches	599	121	655
Branches diameter (μm)	1	1	1

Table 5.1: Morphometric statistics of the original collected trees after processing.

Data Retrieval

In the present study, to determine the effects of electrotonic variability on electrophysiology in neurons, a cerebellum Purkinje, a neocortical layer 5 Pyramidal, and a Visual cortex cell (see Figure 5.1) were obtained from the Neuromorph.org archives [78]. Afterwards, the `.swc` files with the cells topological and metrical information (see Table 5.1) were imported to MATLAB for further processing.

Morphological Noise

Whatever the acquisition and the data processing system, it is difficult to retrieve the real original neuronal structure without errors because of histological, optical and operator-linked distortions. To solve this problem, further processing of the dendritic trees from the collected cells was done using the TREES toolbox [25] trees from MATLAB.

For simplicity in the application of measure e^{-X} and in the analysis of the results, in the present study only neurons with one dendritic tree were considered, therefore the first step of dendritic processing was the removal of the basal dendritic tree from the layer 5

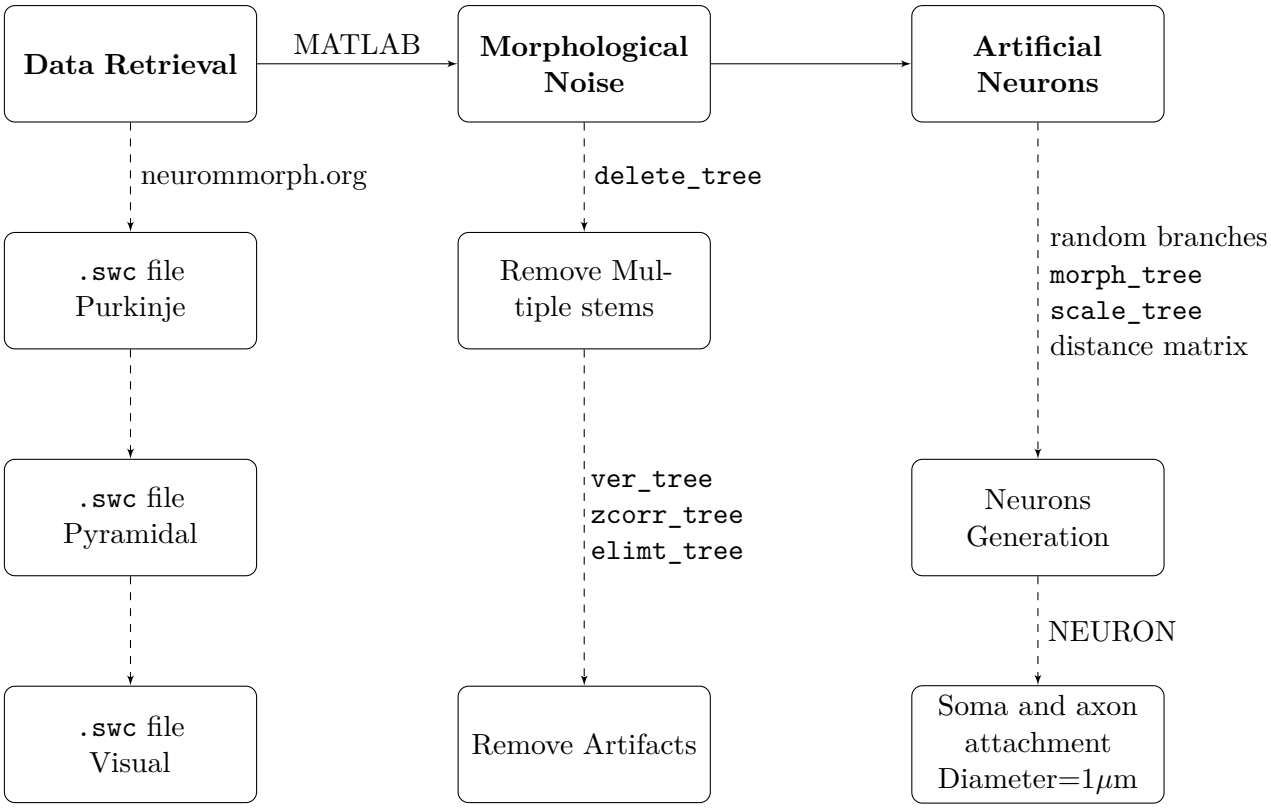

Figure 5.2: Work flow from the cells artificial reconstructions

Pyramidal cell using the function delete_tree from the TREES toolbox. Afterwards, for minimizing the influence of artifacts on the cells geometric and topological information, a series of functions from the TREES toolbox were applied to the dendritic trees, respectively the actions performed were, verification of the integrity of the `.swc` files (`vert_tree`), correction of sudden shifts in the z-axis (`zcorr_tree`), and removal of trifurcations points (`elimt_tree`).

Generation of Artificial Trees

After the integrity of the samples was verified, 27 new dendritic trees were generated, nine from each type, in a total sample $N = 30$. Basically, these new trees only differ from the original ones in terms of the length of its branches, i.e., they maintained the original topology. The first step in the creation of the artificial trees was the generation of new length values for the branches, this was done by creating a uniform random variable over the interval $(0, 20)$ and retrieving samples of numbers that equals the number of branches of each neuron type (see table 5.1). The values found in the previous step were used to create a vector on TREES toolbox environment that replaced the original branch values, using function morph_tree. To maintain the total wiring length the trees were rescaled to their respective the original total wiring length (see Table 5.1) using the scale_tree function. Afterwards, using distance matrix methods, eight new trees were generated for

each type. These new trees' branch lengths lie in between the random and original trees, this was done to create a gradient in terms of (a)symmetry between the random generated trees and the original trees. The final step of this process was accomplished on NEURON software [20], where a soma (length=35μm, diameter=25μm) and an axon (length=110μm, diameter=4μm) were attached to all trees, this was done following the protocol from [70] and [88], and the dendritic branches diameters were equalised to 1 μm.

5.3 Computer Simulations

The models are implemented on NEURON and capture the general features of a real neuron. Standard compartmental modelling techniques were used to simulate spatially extended neurons with passive electrical structure, four voltage-dependent currents: a fast sodium current ($\bar{g}_{Na}$), a slow voltage-dependent non-inactivating potassium current ($\bar{g}_{Km}$), a fast non-inactivating potassium current ($\bar{g}_{Kv}$), a slow calcium-activated potassium current ($\bar{g}_{Kca}$), and a high voltage-activated calcium current ($\bar{g}_{Ca}$); all cells have the same number of evenly distributed ion channels. The cells are activated by dendritic stimulation (see [44]), being stimulated by the same number of excitatory synaptic current that are regularly distributed across the dendritic trees (see Table 5.2). All currents were calculated using conventional Hodgkin-Huxley-style kinetics with an integration time step of 250 μs. For the specific rate functions of each current and respective kinetics schemes, we refer to [70] and [88], or to the `.mod` files in the accompanying cd-ROM.

Before the actual two conditions were simulated, a pre-condition where the electrotonic distances (L_{ij}) were calculated on NEURON software was performed. Then, these values were used to create a MATLAB vector that was morphed to each tree ($N = 30$), creating a tree with the same topological structure of the original ones, but where the metrical parameters were replaced for electrotonic values of each branch.

Axial Current Condition

To test the first hypothesis stated in chapter 3, we investigate how the (a)symmetry of the dendritic trees influences the electrical dynamics of the cells. In this condition, the dendrites from all cells are active (see table 5.2), but the soma and axon are passive, to mimic the blockade of the trigger zone. This is done to make sure that the current reaching the soma was from the dendrites, and not from the opening of the active conductances present in the axo-somatic compartment. Then the synapses are activated once in a synchronous manner, i.e., all at the same time just one time (1Hz), and the axial current is measured at the site where the stem and soma connect. For better resolution, the soma and axon are compartmentalised, each with 9 segments.

	Purkinje			Pyramidal			Visual			
	Dendrites	Soma	Axon	Dendrites	Soma	Axon	Dendrites	Soma	Axon	Units
R_a	80	80	80	80	80	80	80	80	80	Ωcm
C_m	0.75	0.75	0.75	0.75	0.75	0.75	0.75	0.75	0.75	μFcm^{-2}
$\bar{g}_{leak}$	$0.3 * 10^{-5}$	$0.3 * 10^{-5}$	$0.3 * 10^{-5}$	$0.3 * 10^{-5}$	$0.3 * 10^{-5}$	$0.3 * 10^{-5}$	$0.3 * 10^{-5}$	$0.3 * 10^{-5}$	$0.3 * 10^{-5}$	pS μm^{-2}
$\bar{g}_{Na}$	29.4624	0|20	0|30000	20	0|20	0|30000	39.6544	0|20	0|30000	pS μm^{-2}
$\bar{g}_{Km}$	0.1473	0|0.1	0	0.1	0|0.1	0	0.1983	0|0.1	0	pS μm^{-2}
$\bar{g}_{Kv}$	0	0|200	0|2000	0	0|200	0|2000	0	0|200	0|2000	pS μm^{-2}
$\bar{g}_{KCa}$	4.4193	0|3	0	3	0|3	0	5.9482	0|3	0	pS μm^{-2}
$\bar{g}_{Ca}$	0.44193	0|0.3	0	0.3	0|0.3	0	0.59482	0|0.3	0	pS μm^{-2}
d_{syn}	0.000221	0	0	0.00015	0	0	0.000297	0	0	pS μm^{-2}
Δt	250	250	250	250	250	250	250	250	250	μs
Temp	37	37	37	37	37	37	37	37	37	°C
nseg	d_λ	$9\|d_\lambda$	$9\|d_\lambda$	d_λ	$9\|d_\lambda$	$9\|d_\lambda$	d_λ	$9\|d_\lambda$	$9\|d_\lambda$	

Table 5.2: Parameters of the simulations for each neuron in both conditions

Spike Train Condition

In this condition, dendritic tree, soma and axon have active properties. Voltage traces are measured at the axo-somatic compartment to analyse whether differences found at the axial current condition induce differences at the output spiking patterns. The stimulation protocol is similar to the one in the axial current condition, i.e., regular and synchronous, but the synaptic activation frequencies were 1Hz, 4Hz, 7Hz, 10Hz, 20Hz, 50Hz and 100Hz and the regular stimuli were delivered at constant inter-spike intervals corresponding to the input frequency.

5.4 Results and Discussion

Before our initial experiments were conducted, the electrotonic distances of all dendritic branches (L_{ij}) were computed for every neuron ($N = 30$), and were used to create a MATLAB vector that was morphed to each corresponding tree. Specifically, we attempted to match the records for each of the dendritic tree segments present in the NEURON simulation output with the segments in the MATLAB tree description. Due to differences in representation between the two files, a match was not always identified, which we refer to as a parsing error. For nine Purkinje cells, from the total number of branches (599), the number of parsing errors were 3 ± 0 (mean$\pm$s.d.), but one tree got 19 parsing errors, and for this reason it was excluded from the statistical analysis. For the Pyramidal cells, from the total number of branches (121), the parsing errors were 0.4 ± 0.5164, and finally for the Visual cells, from the total number of branches (655), the parsing errors 4.72 ± 4.24.

5.4.1 Axial Current Condition Results

The goal of the first set of simulations was to find support for the synchronization hypothesis stated in section 4.3.1, and particularly, to test the first experimental prediction, which states that more symmetric electrotonic structures will achieve higher levels of current measured at the soma, other things being equal. Taking into account that in these simulations *(i)* the number of synapses, and density of ion channels are the same across all

cells, *(ii)*the total electrotonic distance is constant in each cell type, and *(iii)* the amount of current injected is the same across all cells, the isolation of the symmetry variable is assured.

Furthermore, since intra-cell type have different geometrical arrangements, and each neuron type differs in its total electrotonic distance and topology, one can investigate how size, topology and geometry influence the processing of synaptic inputs in a dendritic tree, while providing a definitive test to the discriminative power of e^{-X}.

After the synapses were activated in a synchronous manner (1Hz), the time-courses of the axial currents reaching the soma were integrated ($\int I_{axial}dt$) and plotted against the e^{-X} values of each tree (see Figure 5.3). For all three different cell types, and across all cell types, the plots could be well fitted[1] ($R^2/\bar{R}^2 > 0.85$) with negative exponential functions ($a * e^{-bx} + c$). The fitting parameters values and residues analysis values for all conditions, are reported in Table 5.3.

Intra-cell Analysis

By analysing the plots (Figure 5.3) from each individual cell type, it is easy to recognize that as e^{-X} decreases, the amount of axial current increases. Since, $e^{-X_{sym}} < e^{-X_{asym}}$, one can interpret these results as an evidence that supports the synchronization hypothesis, as it clearly confirms the first experimental prediction, i.e., more symmetrical structures achieve higher levels of current at the soma. Therefore, structural symmetry seems to play an important role in signal integration, being a possible a mechanism for the modulation of axial current that flows from the dendrites to the soma.

Overall Analysis

In the overall condition, i.e., the analysis of the plot of all cells against all axial current values, the same negative exponential relation between e^{-X} and the quantity of axial current reaching the soma is found. Despite the small differences between values of fitting parameters, the overall shape of the relationships did not change much across conditions (see Figure 5.3), even for the overall condition. Furthermore, the 95% predictive bounds are close to the fitting curve, providing a good indication of the predictive power of the negative exponential model. In addition, the narrow range of fitting parameter values quantitatively confirms this analysis (see Table 5.3).

e^{-X} Analysis

Moreover, e^{-X} was capable of discriminating the structural differences between intra cell types, and across cell types, and these differences highly correlate with functional differences, confirming its discriminative power, and its direct relation between structure

[1]Note that in all conditions, except the Visual condition, have ($R^2/\bar{R}^2 > 0.9$), possibly the lower values for the former condition are caused by the higher number of parsing errors which blured the e^{-X} vs. I_{axial} relation.

	N	Model Type $a * e^{-bx} + c$	SSE	R^2	$\bar{R}^2$	RMSE
Purkinje	9	$7.11 * e^{-0.7566x}$	$1.992e^{-5}$	0.931	0.931	0.001578
Pyramidal	10	$1.924 * e^{-0.6548x}$	$1.854e^{-4}$	0.9313	0.9227	0.004813
Visual	10	$8.144 * e^{-0.3957x} - 0.7$	$6.986e^{-5}$	0.8744	0.8587	0.002955
All cells	29	$7.11 * e^{-1.82x} + 0.26$	$1.624e^{-2}$	0.9891	0.9887	0.02452

Table 5.3: Fitting parameter values and residues analysis for the e^{-X} vs. axial current relation.

and function. This correlation can be attested by the goodness of the fit of the observations (Table 5.3).

Robustness Assessment

In order to evaluate the qualitative and quantitative generality of the proposed synchronization mechanism, i.e., if this mechanism is robust to different conditions, we conducted a thorough analysis on the X factor from e^{-X}. As stated in section 4.3, $X = \sum \frac{w_{rd_1}/w_{rd_2}}{w_{rd_1} + w_{rd_2}}$, the ratio on the numerator assesses the topological and geometrical differences of the dendritic tree, and the sum on the denominator the electrotonic cell's size. Taking this into account, we computed the mean value of $\sum w_{rd_1}/w_{rd_2}$ for each neuron type, and also computed the total electrotonic distance ($\sum w_{ij}$) from each neuron type, interpreting these values as indicators for the overall cell's (a)symmetry and size, respectively. Then these indicators were compared with the average of the integrated axial current time-courses from each cell type.

Regarding the total electrotonic distance the results found were: for the Pyramidal type $\approx$ 489.2 , Purkinje type $\approx$ 2133.8, and Visual type $\approx$ 2178.6. By definition (see section 3.2.3), less signal attenuation was expected for the Pyramidal type, and more attenuation for the Purkinje and Visual type. Therefore, the amount of current reaching the soma for the former should be bigger than for the remaining types, and vice-versa. Nevertheless, the average of the integrated axial current time-courses reaching the soma were: Pyramidal type $\approx$ 1.513 , Purkinje type $\approx$ 4.575, and Visual type $\approx$ 5.43, i.e., the amount of axial current increased when the total electrotonic distance increased as well, which by the electrotonic distance definition does not make sense. However, the the average $\sum w_{rd_1}/w_{rd_2}$ for each cell type follows a similar pattern as the one found at the integrated axial current mean values, with Pyramidal cell types having lower values ($\approx$ 28.11), and the Purkinje ($\approx$ 160.95) and Visual ($\approx$ 140.49) cell types showing bigger and similar higher values, leading one to conclude that the increased axial current was caused by differences in the electrotonic architecture of the cell that override the size effect. These results suggest that current synchronization by structural (a)symmetry is robust to differences to neuronal size across cell types.

Besides size alone, topological and geometrical differences present in neurons, whether

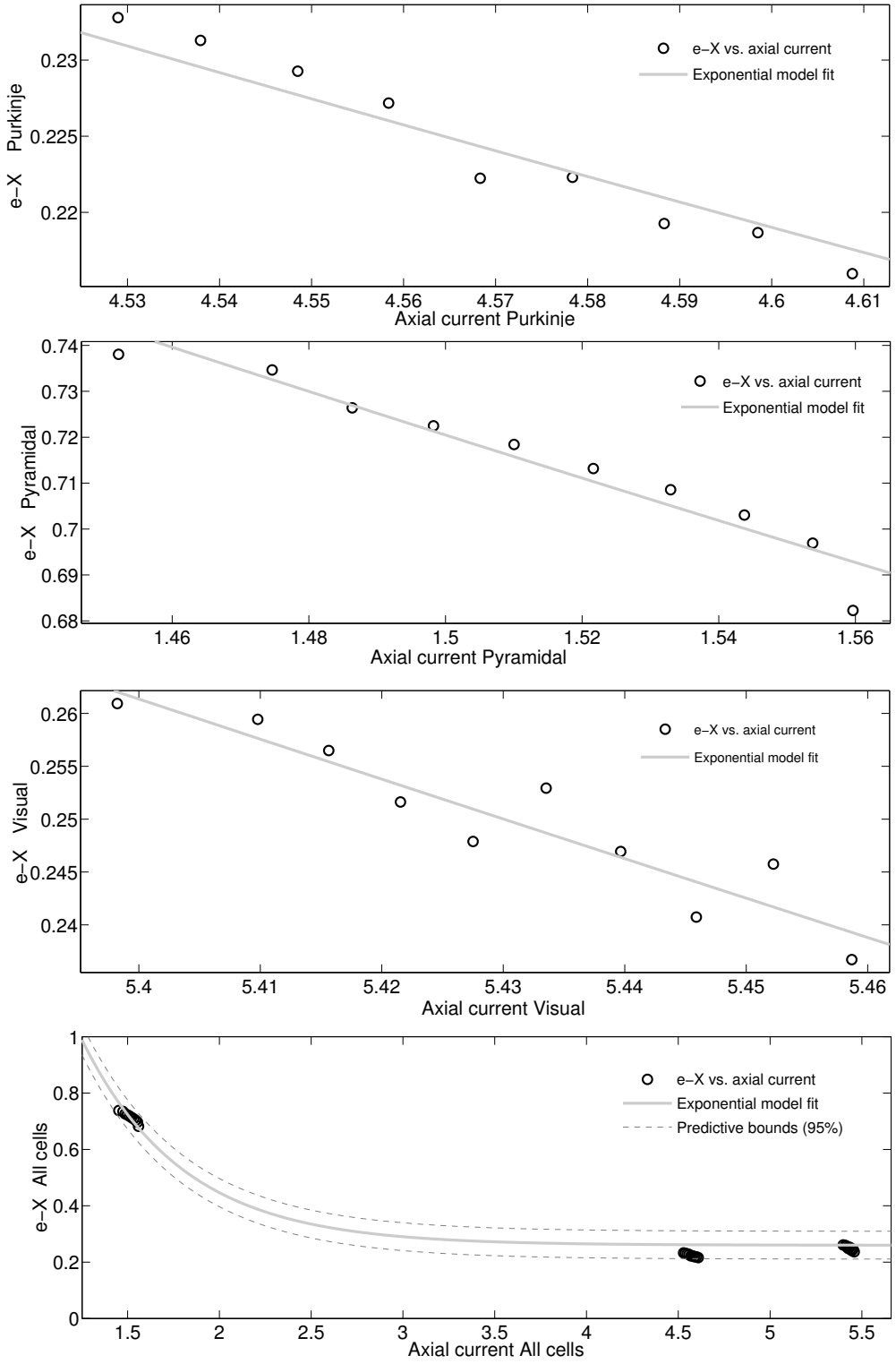

Figure 5.3: Fitting plots for the e^{-X} vs. axial current relation. The neurons within each of the cell types can be well fitted by a negative exponential model with small residuals (see Table 5.3). Since measure e^{-X} is exponentiated, this corresponds to a positive linear fit between the structural factor X and the amount of axial current reaching the soma. Overall, the metric can also be used to predict axial current, based only on structural features, even if the cell type is not known.

from the same type or from different types, have influence on single neurons dynamics and have an important role in dendritic integration [2, 11, 70, 87, 92]. The mechanism(s) behind these differences are poorly known, but from the analysis of the data from the simulation-based experiments performed in this thesis, one can speculate that synchronization can play a role in these long reported physiological differences. With more symmetric structures providing more synchronization, and vice-versa, functioning as a modulatory mechanism that neurons can computationally explore. Additionally, e^{-X} can be used with confidence to quantify those structural differences, while providing a bridge between structure and function. Following these results, e^{-X} can provide valuable insights to the ongoing efforts of correlating dendritic structure and neuronal activity in various cell classes.

5.4.2 Spike Train Condition Results

Different patterns of spike trains, and their precise timing, may have different neurocomputational properties, and cause different responses on the postsynaptic neuron. In order to evaluate whether the heterogeneity of electrical dynamics found in the axial current condition, attributed to variability in the electrotonic structure, influences the output behaviour of single neurons, one main experimental setup was conducted that was analysed in two different ways: *(i)* the amount of time that all neurons took to the exhibit the first spike when stimulated, and *(ii)* the voltage traces were recorded for different input frequencies, to ascertain if the spectrum of firing patterns across cells were different.

Time to Spike Analysis

After the synapses were activated in a synchronous manner (1Hz), the voltage traces of all cells ($N = 29$) were recorded, and the time required to the first spike was measured at the precise moment when the membrane potential reversal happened. One of the recorded observations from a Pyramidal cell was distant from other observations and it was considered an outlier and was removed from further analysis, the remaining observations ($N = 28$) were then plotted against the e^{-X} values of each tree (see Figure 5.4). For all three different cell types, and across all cell types, the plots could be well fitted[2] ($R^2/\bar{R}^2 \gtrsim 0.85$) with exponential functions ($a * e^{bx} + c$). The fitting parameters values and residues analysis values for all conditions, are reported in Table 5.4.

Intra-cell Analysis. By analysing the plots (Figure 5.4) from each individual cell type, it is easy to recognize that as e^{-X} increases, the amount of time required for a cell to spike increases as well. Taking into account the results from the axial current condition, one can interpret these results as an evidence that supports the synchronization hypothesis, as it clearly confirms the second experimental prediction, i.e., more symmetrical structures achieve higher levels of current at the soma, which in turn make a cell reach its threshold sooner than more asymmetrical cells.

[2]Once again, the Visual condition has the lower values of fitness, probably due to the higher number of parsing errors which blurred the e^{-X} vs. time to spike relation.

Overall Analysis. In the overall condition, the same exponential relation between e^{-X} and the amount of time required for a cell to spike is found. Despite the differences between values of fitting parameters, the overall shape of the relationships did not change much across conditions (see Figure 5.4), even for the overall condition.

It is important to note, that the model type used to fit the value is the same as in the axial current condition, making these fits even more credible, and points to a close relation between structure and the time required to a neuron to spike. Once again, the 95% predictive bounds are close to the fitting curve, providing a good indication of the predictive power of the exponential model. In addition, the narrow range of fitting parameter values quantitatively confirms this analysis (see Table 5.4).

Spike Train Analysis

In this condition, all cells ($N = 29$) were activated with the following pre-synaptic frequencies: 1Hz, 4Hz, 7Hz, 10Hz, 20Hz, 50Hz and 100Hz. The stimuli were delivered at constant inter-spike intervals corresponding to the input frequency.

For each cell type, differences on the spike train patterns fail to emerge. For pre-synaptic frequencies ranging from 1-20 Hz, there was no variation between all cells ($N = 29$), with the output frequencies being equal to the input frequencies, i.e., 1Hz±0, 4Hz±0, 7Hz±0, 10Hz±0, 20Hz±0, and the output patterns showed similar inter-spike intervals (see Figure 5.5). Differences on the spike train behaviour only appeared at 50Hz and 100Hz, although these differences were only significant across cell types, and not in intra types. The Purkinje cells showed an average spiking rate of 13Hz±0, 50Hz (mean ± s.d., f_{input}) and 13.8Hz±0.42, 100Hz. Pyramidal cells showed an average spiking rate of 10.9Hz±0.32, 50Hz and 12.9Hz±0.32, 100Hz. Finally, Visual cells showed an average spiking rate of 13Hz±0, 50Hz and 14.2Hz±0.42, 100Hz (see Figure 5.5). General qualitative trends can be drawn from these data, particularly *(i)* cells with similar e^{-X} values have similar output behaviour, and *(ii)* cells with higher e^{-X} values exhibit spike trains with higher frequencies.

Concluding, the electrotonic structure of the cell, measured by e^{-X}, seems to affect the output behaviour of the cell, however, the results found in these simulation-based experiments were not conclusive. We think the results found in the spike train condition were caused by an inadequate stimulation protocol used in these simulations, being homogeneous in space and constant in time. Even though it is an improvement to the somatic stimulation protocol widely used in related works on the field [70, 90], this protocol still is quite artificial when compared with the stochastic pre-synaptic stimulation found in real neurons [67, 68]. We strongly believe, that a more natural activation of synaptic inputs would be expected to exacerbate the influence of morphology on output patterns, and more expressive differences could arise in intra-cell types, and across cell types. Accordingly, this direction should be taken in future work to better support our postulation.

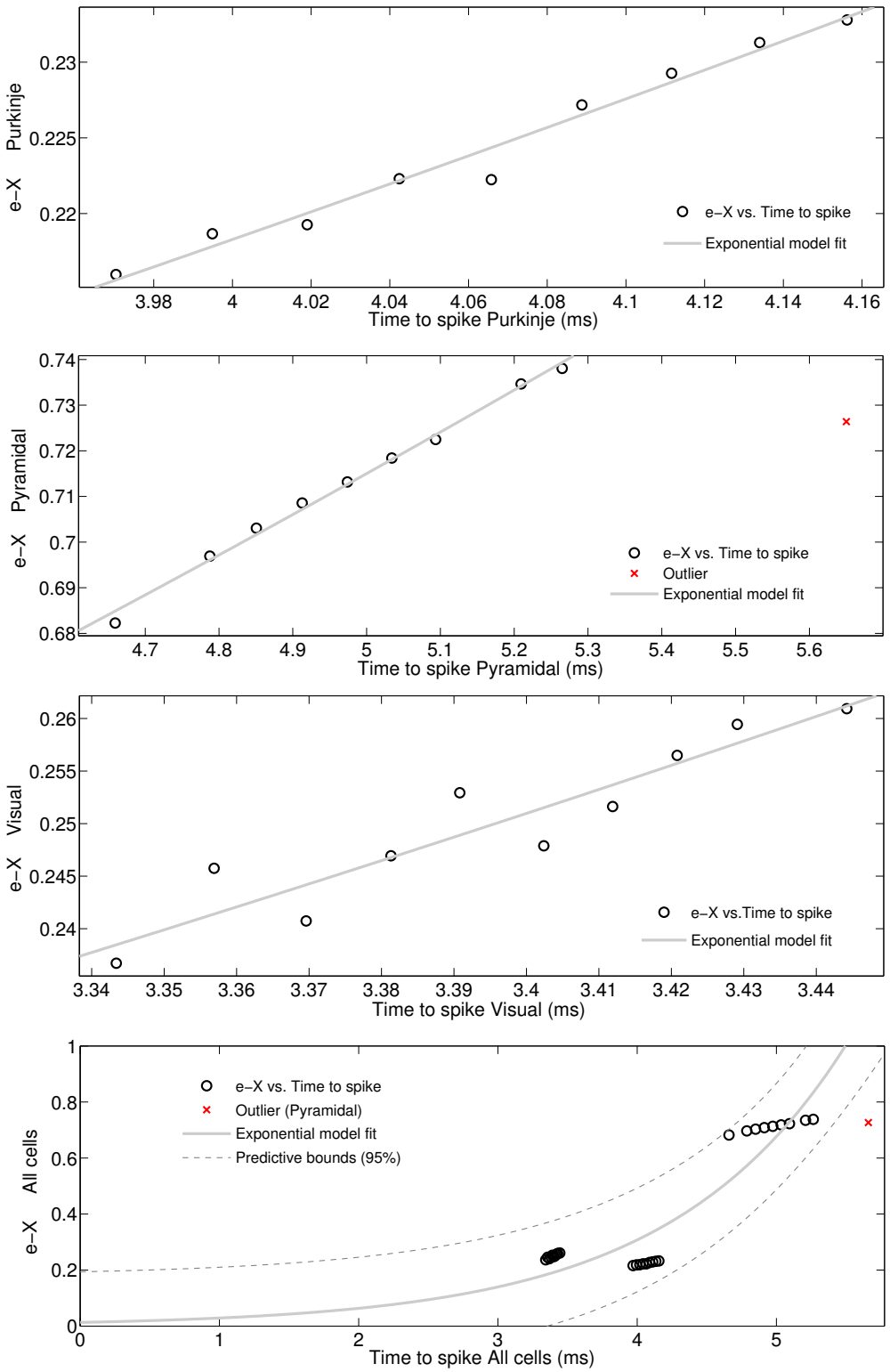

Figure 5.4: Fitting plots for the e^{-X} vs. time to spike relation. The neurons within each of the cell types can be well fitted by an exponential model with small residuals (see Table 5.4). Since measure e^{-X} is exponentiated, this corresponds to a negative linear fit between the structural factor X and the time to first spike. Overall, the metric can also be used to predict the the time required to a neuron to spike , based only on structural features, even if the cell type is not known. This is important because demonstrates a systematic link between neuronal structure and a functional property.

	N	Model Type $a * e^{bx} + c$	SSE	R^2	$\bar{R}^2$	RMSE
Purkinje	9	$0.04121 * e^{0.4168x}$	$6.957e^{-6}$	0.9759	0.9725	0.0009969
Pyramidal	9	$0.3802 * e^{0.1263x}$	$1.494e^{-5}$	0.9941	0.9933	0.001461
Visual	10	$0.01166 * e^{0.9027x}$	$7.146e^{-5}$	0.8715	0.8555	0.002989
All cells	28	$0.01312 * e^{0.7886x}$	0.2006	0.8553	0.8497	0.08783

Table 5.4: Fitting parameter values and residues analysis for the e^{-X} vs. time to spike.

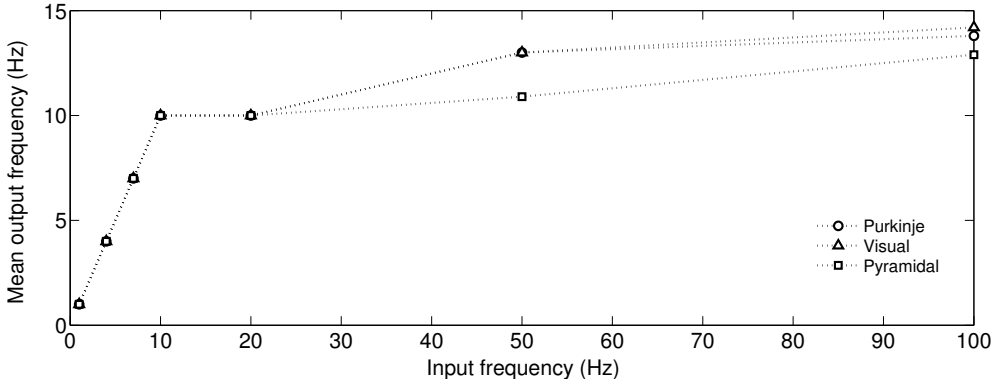

Figure 5.5: Average spiking rate plot for the three cell types. Cells with similar e^{-X} values (Purkinje and Visual) have similar output behaviour, and cells with higher e^{-X} values (Purkinje and Visual) exhibit spike trains with higher frequencies.

5.5 Summary

In this chapter, we described the simulation-based experiments used to test the synchronization hypothesis, and to test the discriminative power of e^{-X}. First, we started by indicating the methods used in the artificial reconstructions of the simulated cells, then a description of the simulations ensued. Regarding the experimental results, we highlight a number of points. **First**, our results demonstrate how the electrotonic structure of a neuron may shape the electrical dynamic interactions in single neurons. Particularly, support for the synchronization hypothesis was found, as the first experimental prediction was confirmed. **Second**, the results analysis led to the confirmation of the methodological prediction , and e^{-X} can be used with confidence to quantify those structural differences, while providing a bridge between structure and function. **Third**, the second experimental condition was inconclusive, as significant differences fail to emerge in some conditions. Nevertheless, this may be accounted by some limitations in the stimulation protocol. Overall, the results show that measure e^{-X} is a promising alternative to traditional morphometrics measures as it can be used with confidence to quantify structural differences, and can be applied across different types of neurons while providing a bridge between structure and function.

Chapter 6

Conclusions

In this chapter we summarise the contributions of the dissertation, and discuss directions for future work, and possible extensions, improvements and refinements that the work done here could still benefit from. A brief conclusion ensues.

6.1 Summary and Contributions

We consider that the objectives defined in section 1.2 were reached. We have developed a new measure that quantitatively accounts for variations in metrical, topological and biophysical components of the cell all at the same time, and because the way it is defined it has shown a highly discriminative power (see section 4.3). Other efforts in the literature could only account for just one of these parameters at a time (e.g., the partition asymmetry index [91]) and undoubtedly those measures cannot sufficiently characterize dendritic structure. e^{-X} on the other hand, came to fill the need for a measure that could provide a link between geometry, topology and function, and the results analysis lead us to conclude that it can be used with confidence to quantify those structural parameters.

Before e^{-X}, because of the methodological hindrance supra mentioned, the effects of dendritic size, topology, geometry, and its underlying mechanisms, on neuronal dynamics remained poorly known. This situation was exacerbated by some methodological flaws, such as the use of the less appropriate stimulation protocol of somatic current injection in simulation-based experiences [70, 90]. To overcome this, we used e^{-X} to systematically investigate how synaptic efficacy is affected by the anatomical and biophysical properties of the postsynaptic cell, particularly, how the physical parameters controlled by dendritic morphology underlies the differences in the electrical dynamics of the cell.

We proposed and tested the synchronization hypothesis, which states a new mechanism that neurons can explore to process PSPs (see section 4.3.1). Basically, the combination of topological, metrical and biophysical structural components of a neuron emerge a specific electrotonic structure of that particular cell. The more symmetric this structure is, the more similar the electrical behaviour of the cell will be, i.e., the current flowing from different paths will have similar dynamics, and consequently will spatially sum in a more

efficient way. Therefore, structural differences may serve as mechanism for modulating axial current that flows from the dendrites to the soma that influence the output behaviour of the cell.

Support for the synchronization hypothesis was found, as more symmetric electrotonic structures achieved higher levels of current measured at the soma compared with asymmetrical structures, when injected with the same current. Moreover, on the second experimental condition the synchronization hypothesis enjoyed some support, as differences found in the axial current condition correlated with the time that neurons required to spike, with more symmetrical neurons requiring less time to do so. Nevertheless, significant differences fail to emerge in the output spike trains, but these results can be explained by some limitations in the stimulation protocol and needs further analysis in the future (see section 5.4).

6.2 Future Work

In this section, we describe possible future developments for e^{-X}, and to the methods used to test the synchronization hypothesis. The subsections presented overview three main areas of future work, namely: *(i)* new stimulation protocol, *(ii)* using the new differential equations solver CVode, and *(iii)* try to validate the results found here in a bigger and broader range of neurons.

New Stimulation Protocol

The stimulation protocol used in these simulations was not the most adequate since it was homogeneous in space and constant in time. Even though it represents an improvement to the somatic stimulation protocol widely used in related works on the field [70, 90], it is still quite artificial when compared with the random and asynchronous kind of pre-synaptic [67, 68] stimulation found in biological neurons. We strongly believe that a more natural activation of synaptic inputs would be expected to exacerbate the influence of morphology on output patterns, and more expressive differences could arise in intra-cell types, and across cell types, specially in what regards the output behaviour of the cell. This is a crucial development that the work done here could still benefit from.

Code Optimization

NEURON software has recently been upgraded with a new built-in differential equations solver named CVode, which is a multi order variable time step integration method [20]. One of the main reasons why this new solver was integrated on NEURON was the necessity to increase the accuracy of the electrotonic distance computation. However, most `.mod` files containing the ion channels's kinetics schemes found on the literature, particularly the ones used in this thesis, are not compatible with this new integrator and need to be generalized to enjoy these performance benefits. Although it is hard to tell exactly by how

much, it is conceivable that this new integrator could greatly increase the accuracy of the electrotonic distance computation making the structure-function relation more clear.

Bigger Sample and Applications

Probably the most obvious extension that the work done in this study could benefit from is conduct the simulation-based experiments on a larger and eclectic sample of neurons. This would provide a bigger statistical power, and would enable the validation of the results found in the present manuscript, and further test the predictive of e^{-X}.

On a different note, this large neuronal sample could be used for a systematic account of different neuron cell types. Since the neuron classification is a basic prerequisite for understanding the nervous system functional patterns, measure e^{-X} could provide a helpful tool for the explicit classification of known neuron types into functional classes [15]. Particularly, one possible and interesting translational application for measure e^{-X} would be the study and prediction of structural aberrant cells behaviour [57, 66, 93].

6.3 Overview

Only a few years ago, the brain computational power was seen only as the result of network connectivity, and in this perspective, single neurons were no more than an passive integrator devices [73]. Nowadays, individual neurons are seen as extremely complex structures, that perform many kinds of computations, and dendrites with theirs morphological diversity clearly play an important role in information processing [69]. These structural differences make the basis for differences in electrical dynamics of single neurons [24].

It is known that neuroanatomical variability has an effect on the neuronal response, and numerous studies attempted to quantify these effects, some of them tried to vary and analyse metrical features of dendritic trees holding the rest of the parameters [61, 62, 64, 63, 65], while other studies tried a different approach and varied the topological features of a dendritic tree [30, 88, 89]. Some have made an effort to isolate the effect of morphology from variations in physiology, while other studies have done just the opposite and altered the physiology to overcome differences in morphology [48]. In all cases, variations in shape, ionic channel composition, even within the same cell class, caused variations in the electrical dynamics of the cell and in neuronal responses. Even though all these data that has been accumulated, few mechanisms have been proposed that relate structure to function [24].

Synchronization Mechanism and Single Neurons

If we accept that the artificial conditions of our simulation-based experiments mimic different states of neuronal activity, the synchronization mechanism proposed in this manuscript may be at least one structure based mechanism that neurons can exploit computationally. But how?

One specific example where neurons can benefit from the synchronization mechanism may be found in **sensory neurons** [56]. For example, a neuron might be driven by an external stimulus which is suddenly switched on, this may happen in a realistic situation where abrupt changes in the environment are quite common, as for instance when the photoreceptors in the retina receive a new visual input. The processing of an abrupt change from a noisy environment may have crucial biological and adaptive relevance, as it may be a predator, an hazardous object, etc., consequently, information about the onset of that particular stimulus needs to be quickly and reliably available in the brain for further processing [56]. Therefore, we can imagine a code where the precise timing of the first spike after the reference signal has tremendous importance [37]. To obtain a quick and reliable response to an input, a more symmetrical electrotonic structure may increase the synchronization of the current released due to the signal transduction, consequently increasing the amount of current reaching the soma, making the probability of a neuron to spike increase, and the time required to spike decrease.

Back to the Network

Although neurons are powerful computational devices they have limitations [59], and to put neurons back into networks is the ultimate step for the comprehension of the nervous system. One important task is to explore how different neuron types, with their different structures interact with each other in the network, showing how specific emergent behaviours such as synchronization and oscillations arise, and how these observed phenomenon underlie information processing [7, 94].

6.4 Conclusion

This thesis showed that measure e^{-X} is a promising alternative to traditional morphometrics measures as it can be used with confidence to quantify structural differences, and can be applied across different types of neurons while providing a bridge between structure and function. This was empirically demonstrated with two different simulation-based experiments, where e^{-X} discriminated different neuronal structures and at the same time correlated with different relevant functional properties of the modelled cells. Our contributions represent a new step in the iterating loop of model prediction, experimental test, and model adjustment that hopefully will allow us to correlate neuronal structure to function then to behaviour, providing a deeper understanding of how single neurons structure contribute to computation in the brain.

Appendix A

Measures Comparison

In this appendix, we introduce a sort of benchmark for different morphometric measures and e^{-X} . The chosen measures are used in many different studies and are representative of topological and metrical morphometrics (see section 3.2.1). This analysis strictly evaluates the discriminative power of the three analysed measures, and it is not concerned about on how they are applied in the literature, or on how they are derived.

The Measures

The analysed measures were the following:

- **Topological asymmetry** [24, 88, 89, 91] - It is a topological measure which characterizes the binary tree as the mean value of all its A_p (see section 3.2.1), ranging from $j = 1$ to $j = n - 1$, where $n - 1$ is the number of branching points. The partition asymmetry values ranges from 0 (completely symmetric) to 1 (completely asymmetric), and it is defined in the following way:

$$A_t = \frac{1}{n-1} \sum_{j=1}^{n-1} A_{p_j} \tag{A.1}$$

- **Mean path length** [8, 82, 89] - The mean path length is the sum of all dendritic path lengths measured from tip to soma divided by the number of terminal segments and it evaluates the overall metrical size. Thus, for a given tree with n terminal segments, the mean path length P_t is:

$$P_t = \frac{1}{n} \sum_{j=1}^{n} P_j \tag{A.2}$$

- e^{-X}- See section 4.3.1.

Toy Models

For a systematic evaluation of the measures discriminative power, we used a set of 23 neurons consisting of all the topologically different trees with eight terminal segments and

Figure A.1: All the different degree eight topologies. For display purposes, some segments have been lengthened, but all segments have the same length in the analysis.

sixteen nodes (see figure A.1). The trees may be thought of as representing the backbones of potentially larger dendritic arborizations. All segments in the tree, intermediate and terminal segments, have the same length ($l = 1$), so the different tree topologies do not differ in total dendritic length.

Results

The results found are reported in table A.1[1]:

	Topological Asymmetry	Mean Path Length	e^{-X}
1	0.86	5.375	0.90326
2	0.67	4.750	0.75336
3	0.66	4.875	0.80156
4	0.64	5.000	0.80399
5	0.62	5.125	0.81701
6	0.62	4.375	0.74260
7	0.60	4.625	0.76447
8	0.57	4.875	0.74394
9	0.57	4.250	0.89405
10	0.57	5.250	0.82633
11	0.45	4.375	0.65040
12	0.43	4.500	0.66635
13	0.42	4.625	0.69419
14	0.38	4.125	0.76305
15	0.38	4.250	0.65990
16	0.38	4.625	0.70522
17	0.37	4.750	0.72755
18	0.36	4.875	0.74198
19	0.33	4.250	0.67798
20	0.31	4.500	0.69417
21	0.29	4.125	0.61714
22	0.17	4.250	0.56967
23	0	4.000	0.51879

Table A.1: Measures comparison results. Trees are organized accordingly to Figure A.1, being number 1 the leftmost tree and 23 the rightmost tree. The topological asymmetry measure could not discriminate three sets of trees from each other (5, 6); (8, 9, 10); (14, 15, 16). The mean path length measure could not discriminate six sets of trees (2, 17); (3, 8, 18); (6, 11); (7, 13, 16); (9, 15, 19, 22); (12, 20). On the other hand, e^{-X} could discriminate all trees.

[1]Only the first five decimal places of e^{-X} are shown table A.1.

Bibliography

[1] H Agmon-Snir, CE Carr, and J Rinzel. The role of dendrites in auditory coincidence detection. *Nature*, 393(May), 1998.

[2] Joseph M Amatrudo, Christina M Weaver, Johanna L Crimins, Patrick R Hof, Douglas L Rosene, and Jennifer I Luebke. Influence of highly distinctive structural properties on the excitability of pyramidal neurons in monkey visual and prefrontal cortices. *The Journal of neuroscience : the official journal of the Society for Neuroscience*, 32(40):13644–60, October 2012.

[3] P Andersen, R Morris, D Amaral, T Bliss, and J O'Keefe. *The Hippocampus Book*. 2006.

[4] Mogens Andreasen and JD Lambert. Regenerative properties of pyramidal cell dendrites in area ca1 of the rat hippocampus. *The Journal of Physiology*, 483(Pt 2):421–441, 1995.

[5] Mogens Andreasen and John DC Lambert. The excitability of ca1 pyramidal cell dendrites is modulated by a local calcium-dependent potassium-conductance. *Brain research*, 698(1):193–203, 1995.

[6] MA Arbib and JS Grethe. *Computing the brain: a guide to neuroinformatics*. Number 71. Academic Press, 2001.

[7] Alex Arenas, Albert Díaz-Guilera, Jurgen Kurths, Yamir Moreno, and Changsong Zhou. Synchronization in complex networks. *Physics Reports*, 469(3):93–153, December 2008.

[8] Giorgio a. Ascoli. *Computational Neuroanatomy: Principles and Methods*. Humana Press, New Jersey, July 2002.

[9] RC Barr and R Plonsey. *Bioelectricity: A Quantitative Approach*. Springer-Verlarg, 2007.

[10] LW Beineke and RJ Wilson. *Topics in algebraic graph theory*. Cambridge University Press, 2004.

[11] John M Bekkers and Michael Häusser. Targeted dendrotomy reveals active and passive contributions of the dendritic tree to synaptic integration and neuronal output. *Proceedings of the National Academy of Sciences of the United States of America*, 104(27):11447–52, July 2007.

[12] S Boccaletti, V Latora, Y Moreno, M Chavez, and D Hwang. Complex networks: Structure and dynamics. *Physics Reports*, 424(4-5):175–308, February 2006.

[13] B Bollobás. *Modern graph theory*. Springer, 1998.

[14] JA Bondy and USR Murty. *Graph theory with applications*. Elsevier, 1976.

[15] Mihail Bota and Larry W Swanson. The neuron classification problem. *Brain research reviews*, 56(1):79–88, November 2007.

[16] James M. Bower and David Beeman. *The Book of GENESIS: Exploring Realistic Neural Models with the GEneral NEural SImulation System*. Springer New York, 2003.

[17] Paul C Bressloff. *Waves in Neural Media From Single neurons to neural fields*. 2014.

[18] R C Cannon, H V Wheal, and D a Turner. Dendrites of classes of hippocampal neurons differ in structural complexity and branching patterns. *The Journal of comparative neurology*, 413(4):619–33, November 1999.

[19] Nicholas T Carnevale, New Haven, Brenda J Claiborne, San Antonio, Kenneth Y Tsai, and Thomas H Brown. The Electrotonic Transformation: a Tool for Relating Neuronal Form to Function. 7:1–9, 1995.

[20] NT Carnevale and ML Hines. *The NEURON book*. Oxford University Press, Oxford, UK, 2006.

[21] R Cazé, MD Humphries, and BS Gutkin. Spiking and saturating dendrites differentially expand single neuron computation capacity. *NIPS*, pages 1–9, 2012.

[22] Wanpracha Chaovalitwongse. *Computational neuroscience*. Springer-Verlag, 2010.

[23] Wai-Kai Chen. *Graph theory and its engineering applications*. World Scientific, 1997.

[24] Hermann Cuntz. *The Computing Dendrite- From Structure to Function*, volume 11 of *Springer Series in Computational Neuroscience*. Springer New York, New York, NY, 2014.

[25] Hermann Cuntz, Friedrich Forstner, Alexander Borst, and Michael Häusser. The TREES toolbox—probing the basis of axonal and dendritic branching. *Neuroinformatics*, pages 91–96, 2011.

[26] Hermann Cuntz, Friedrich Forstner, Bettina Schnell, Georg Ammer, Shamprasad Varija Raghu, and Alexander Borst. Preserving neural function under extreme scaling. *PloS one*, 8(8):e71540, January 2013.

[27] P Dayan and LF Abbott. *Theoretical neuroscience: computational and mathematical modeling of neural systems*. MIT Press, Cambridge, Massachusetts, 2003.

[28] N Deo. *Graph theory with applications to engineering and computer science*. Prentice-Hall, Inc., 1974.

[29] Mildred Dresslhaus, Gene Dresselhaus, and Ado Jorio. *Group Theory Application to the Physics of Condensed Matter*. Springer, 2008.

[30] Jacob Duijnhouwer, MWH Remme, Arjen Van Ooyen, and J van Pelt. Influence of dendritic topology on firing patterns in model neurons. *Neurocomputing*, 40:183–189, 2001.

[31] J Ehlers, K Hepp, and H Weidenmu. *Symmetry, Group Theory, and the Physical Properties of Crystals*. Springer, 2010.

[32] GB Ermentrout. *Tutorials in Mathematical Biosciences I*. Springer-Verlarg, 2005.

[33] GB Ermentrout and DH Terman. *Mathematical foundations of neuroscience*. Springer-Verlarg, 2010.

[34] Dario Floreano and Claudio Mattiussi. *Bio-inspired artificial intelligence: theories, methods, and technologies*. MIT Press, Cambridge, Massachusetts, 2008.

[35] Michael D. Forrest. Intracellular calcium dynamics permit a Purkinje neuron model to perform toggle and gain computations upon its inputs. *Frontiers in Computational Neuroscience*, 8(August):1–19, August 2014.

[36] LR Foulds. *Graph theory applications*. Springer, 1992.

[37] Wulfram Gerstner and Werner Kistler. *Spiking Neurons Models, Single Neurons, Populations and Plasticity*. Cambridge University Press, Cambridge, UK, 2002.

[38] Marc-Oliver Gewaltig and Markus Diesmann. Nest (neural simulation tool). *Scholarpedia*, 2(4):1430, 2007.

[39] CD Godsil and G Royle. *Algebraic graph theory*. Springer, 2001.

[40] AE Gonzalez. Introductory graph theory for electrical and electronics engineers. *IEEE Multidisciplinary Engg. Edu. Magz*, 2(2):5–13, 2007.

[41] B Graham, A Gillies, and D Willshaw. *Principles of computational modelling in neuroscience*. Cambridge University Press, 2011.

[42] JL Gross and J Yellen. *Handbook of graph theory*. CRC Press LLC, 2004.

[43] S Grün and S Rotter. *Analysis of parallel spike trains*. Springer, 2010.

[44] Antoni Guillamon, David W McLaughlin, and John Rinzel. Estimation of synaptic conductances. *Journal of physiology, Paris*, 100(1-3):31–42, 2006.

[45] Allan T Gulledge, Björn M Kampa, and Greg J Stuart. Synaptic integration in dendritic trees. *Journal of neurobiology*, 64(1):75–90, July 2005.

[46] Onder Gürcan, Kemal S Türker, Jean-Pierre Mano, Carole Bernon, Oğuz Dikenelli, and Pierre Glize. Mimicking human neuronal pathways in silico: an emergent model on the effective connectivity. *Journal of computational neuroscience*, July 2013.

[47] Maryam Halavi, Kelly a Hamilton, Ruchi Parekh, and Giorgio a Ascoli. Digital reconstructions of neuronal morphology: three decades of research trends. *Frontiers in neuroscience*, 6(April):49, January 2012.

[48] Etay Hay, Felix Schürmann, Henry Markram, and Idan Segev. Preserving axosomatic spiking features despite diverse dendritic morphology. *Journal of neurophysiology*, 109(12):2972–81, June 2013.

[49] Andreas V M Herz, Tim Gollisch, Christian K Machens, and Dieter Jaeger. Modeling Single-Neuron Dynamics Detail and Abstraction. *Science*, 314(October):80–85, 2006.

[50] Giacomo Indiveri, Bernabé Linares-Barranco, Tara Julia Hamilton, André van Schaik, Ralph Etienne-Cummings, Tobi Delbruck, Shih-Chii Liu, Piotr Dudek, Philipp Häfliger, Sylvie Renaud, Johannes Schemmel, Gert Cauwenberghs, John Arthur, Kai Hynna, Fopefolu Folowosele, Sylvain Saighi, Teresa Serrano-Gotarredona, Jayawan Wijekoon, Yingxue Wang, and Kwabena Boahen. Neuromorphic silicon neuron circuits. *Frontiers in neuroscience*, 5(May):73, January 2011.

[51] EM Izhikevich and J Moehlis. *Dynamical Systems in Neuroscience: The geometry of excitability and bursting*. The MIT Press, 2008.

[52] Eugene M Izhikevich. Neural Excitability , Spiking and Bursting. *International Journal of Bifurcation and Chaos*, 10(6):1171–1266, 2000.

[53] Eugene M Izhikevich, Niraj S Desai, Elisabeth C Walcott, and Frank C Hoppensteadt. Bursts as a unit of neural information: selective communication via resonance. *Trends in neurosciences*, 26(3):161–7, March 2003.

[54] Morten S Jensen and Yoel Yaari. Role of intrinsic burst firing, potassium accumulation, and electrical coupling in the elevated potassium model of hippocampal epilepsy. *Journal of neurophysiology*, 77(3):1224–1233, 1997.

[55] J Jost. *Mathematical methods in biology and neurobiology*. Springer, 2014.

[56] Eric R Kandel, James H Schwartz, Thomas M Jessell, Sarah Mack, Jane Dodd, John Butler, Harriet Lebowitz, Shirley Dahlgren, Production Supervisor, Eve Siegel, Art Manager, Joellen Ackerman, Judy Cuddihy, Precision Graphics, and R R Donnelley. *Principles of Neural Science*. McGraw-Hill Medical, 4 edition, 2002.

[57] Haruo Kasai, Masahiro Fukuda, Satoshi Watanabe, Akiko Hayashi-Takagi, and Jun Noguchi. Structural dynamics of dendritic spines in memory and cognition. *Trends in neurosciences*, 33(3):121–9, March 2010.

[58] Hojeong Kim and Kelvin E Jones. Asymmetric electrotonic coupling between the soma and dendrites alters the bistable firing behaviour of reduced models. *Journal of computational neuroscience*, 30(3):659–74, June 2011.

[59] C Koch and I Segev. The role of single neurons in information processing. *Nature neuroscience*, 3 Suppl:1171–7, November 2000.

[60] Christof Koch. *Biophysics of computation: information processing in single neurons*. Oxford University Press, Oxford, UK, 1st edition, 2004.

[61] S M Korogod and I B Kulagina. Geometry-induced features of current transfer in neuronal dendrites with tonically activated conductances. *Biological cybernetics*, 79(3):231–40, September 1998.

[62] Sergey M Korogod. Electro-geometrical coupling in non-uniform branching dendrites. 93:85–93, 1996.

[63] Sergey M Korogod and Anton V Kaspirzhny. Spatial heterogeneity of passive electrical transfer properties of neuronal dendrites due to their metrical asymmetry. *Biological cybernetics*, 105(5-6):305–17, December 2011.

[64] Sergiy Mikhailovich Korogod and Suzanne Tyč-Dumont. *Electrical Dynamics of the Dendritic Space*. Cambridge University Press, Cambridge, 2009.

[65] I B Kulagina, S M Korogod, G Horcholle-Bossavitt, C Batini, and S Tyc-Dumont. The electro-dynamics of the dendritic space in Purkinje cells of the cerebellum. *Archives italiennes de biologie*, 145(3-4):211–33, November 2007.

[66] Vaishali a Kulkarni and Bonnie L Firestein. The dendritic tree and brain disorders. *Molecular and cellular neurosciences*, 50(1):10–20, May 2012.

[67] Xiaoshen Li and Giorgio a Ascoli. Computational simulation of the input-output relationship in hippocampal pyramidal cells. *Journal of computational neuroscience*, 21(2):191–209, October 2006.

[68] Xiaoshen Li and Giorgio a Ascoli. Effects of synaptic synchrony on the neuronal input-output relationship. *Neural computation*, 20(7):1717–31, July 2008.

[69] Michael London and Michael Häusser. Dendritic computation. *Annual review of neuroscience*, 28:503–32, January 2005.

[70] Z F Mainen and T J Sejnowski. Influence of dendritic structure on firing pattern in model neocortical neurons. *Nature*, 382(6589):363–6, July 1996.

[71] Klaus Mainzer. Symmetry and complexity in dynamical systems. *European Review*, 13(S2):29, August 2005.

[72] Henry Markram. The blue brain project. *Nature reviews. Neuroscience*, 7(2):153–60, February 2006.

[73] WS McCulloch and W Pitts. A logical calculus of the ideas immanent in nervous activity. *The bulletin of mathematical biophysics*, 5:115–133, 1943.

[74] Brendan D. McKay and Adolfo Piperno. Practical graph isomorphism, II. *Journal of Symbolic Computation*, 60:94–112, January 2014.

[75] M Migliore, EP Cook, DB Jae, DA Turner, and D Johnston. Computer simulations of morphologically reconstructed ca3 hippocampal neurons. *Journal of neurophysiology*, 73(3), 1995.

[76] MF Moody. *Structural Biology Using Electrons and X-rays: An Introduction for Biologists*. 2011.

[77] Randall C. O'Reilly, Yuko Munakata, Michael J. Frank, Thomas E. Hazy, and Contributors. *Computational Cognitive Neuroscience*. Wiki Book, 1st Edition, URL: `http://ccnbook.colorado.edu`, 2012.

[78] Ruchi Parekh and Giorgio a Ascoli. Neuronal morphology goes digital: a research hub for cellular and system neuroscience. *Neuron*, 77(6):1017–38, March 2013.

[79] Simon P Peron, Holger G Krapp, and Fabrizio Gabbiani. Influence of electrotonic structure and synaptic mapping on the receptive field properties of a collision-detecting neuron. *Journal of neurophysiology*, 97(1):159–77, January 2007.

[80] Marta Rivera-Alba, Shiv N Vitaladevuni, Yuriy Mishchenko, Yuriy Mischenko, Zhiyuan Lu, Shin-Ya Takemura, Lou Scheffer, Ian a Meinertzhagen, Dmitri B Chklovskii, and Gonzalo G de Polavieja. Wiring economy and volume exclusion determine neuronal placement in the Drosophila brain. *Current biology : CB*, 21(23):2000–5, December 2011.

[81] Marco B L Rocchi, Davide Sisti, Maria Cristina Albertini, and Laura Teodori. Current trends in shape and texture analysis in neurology: aspects of the morphological substrate of volume and wiring transmission. *Brain research reviews*, 55(1):97–107, August 2007.

[82] Alexei V Samsonovich and Giorgio A Ascoli. Statistical morphological analysis of hippocampal principal neurons indicates cell-specific repulsion of dendrites from their own cell. *Journal of neuroscience research*, 71(2):173–187, 2003.

[83] Idan Segev, John Rinzel, and Gordon M Shepherd. *Theoretical Foundations of Dendritic Function*. MIT Press, 1 edition, 1994.

[84] Nelson Spruston, Greg Stuart, and Michael Häusser. Dendritic Integration. In *Dendrites*, chapter 14. Oxford University Press, 2008.

[85] Nelson Spruston, Greg Stuart, and Michael Häusser. Evolution and scaling of dendrites. In *Dendrites*, chapter 2. Oxford University Press, 2008.

[86] Naoya Takahashi, Kazuo Kitamura, Naoki Matsuo, Mark Mayford, Masanobu Kano, Norio Matsuki, and Yuji Ikegaya. Locally synchronized synaptic inputs. *Science (New York, N.Y.)*, 335(6066):353–6, January 2012.

[87] Benjamin Torben-Nielsen and Klaus M Stiefel. An inverse approach for elucidating dendritic function. *Frontiers in computational neuroscience*, 4(September):128, January 2010.

[88] Ronald a J van Elburg and Arjen van Ooyen. Impact of dendritic size and dendritic topology on burst firing in pyramidal cells. *PLoS computational biology*, 6(5):e1000781, May 2010.

[89] Arjen van Ooyen, Jacob Duijnhouwer, Michiel W H Remme, and Jaap van Pelt. The effect of dendritic topology on firing patterns in model neurons. *Network (Bristol, England)*, 13(3):311–25, August 2002.

[90] J Van Pelt and AK Schierwagen. Electrotonic properties of passive dendritic trees-effect of dendritic topology. *Progress in brain research*, 102:127–127, 1994.

[91] J Van Pelt, H B Uylings, R W Verwer, R J Pentney, and M J Woldenberg. Tree asymmetry–a sensitive and practical measure for binary topological trees. *Bulletin of mathematical biology*, 54(5):759–84, September 1992.

[92] P Vetter, a Roth, and M Häusser. Propagation of action potentials in dendrites depends on dendritic morphology. *Journal of neurophysiology*, 85(2):926–37, February 2001.

[93] Stephen Waxman. *Clinical neuroanatomy*. McGraw-Hill Companies, inc., 2010.

[94] Bruce J. West, Elvis L. Geneston, and Paolo Grigolini. Maximizing information exchange between complex networks. *Physics Reports*, 468(1-3):1–99, October 2008.

[95] M Zador and San Diego. The Morphoelectrotonic Dendritic Function Transform : Approach to Dendritic Structure. 15(March):1669–1682, 1995.